

# Sustainable Energy & Fuels

Interdisciplinary research for the development of sustainable energy technologies

[rsc.li/sustainable-energy](https://rsc.li/sustainable-energy)





ISSN 2398-4902



Cite this: *Sustainable Energy Fuels*,  
2021, 5, 604

## Alkaline membrane fuel cells: anion exchange membranes and fuels

Maša Hren,<sup>a</sup> Mojca Božič,<sup>b</sup> Darinka Fakin,<sup>a</sup> Karin Stana Kleinschek <sup>cd</sup>  
and Selestina Gorgieva <sup>\*ac</sup>

Alkaline anion exchange membrane fuel cells (AAEMFC) are attracting ever-increasing attention, as they are promising electrochemical devices for energy production, presenting a viable opponent to the more researched proton exchange membrane fuel cells (PEMFCs). Consequently, great progress has been made in the area of designing and developing synthetic or naturally-derived anion exchange membrane (AEM), the properties of which have been discussed in this review, *i.e.* ionic conductivity, ion exchange capacity, fuel crossover, durability, stability and cell performance. Major groups of natural polymers (*e.g.* chitosan (CS)) and nanocellulose, together with modification/crosslinking routes, have been mentioned as more ecologically and economically viable raw materials for AEM processing compared to synthetic ones. Performances of fuel cells are also discussed, with different fuels used as anode feeds. Although the AEMFC technology is promising, the longevity challenges remain, originating from the still-limited long-term stability of hydroxide-conducting ionomers, particularly when operating at higher cell temperatures.

Received 12th September 2020  
Accepted 15th November 2020

DOI: 10.1039/d0se01373k

rsc.li/sustainable-energy

### 1. Introduction

In response to global pollution, associated mainly with fossil fuels use, utilising new ways in energy generation and conversion have been a major challenge in the past decades.<sup>1</sup> Fossil fuels are still the most used source for providing energy, resulting in environmental pollution and greenhouse gas emission, especially gases such as CO<sub>2</sub> and CO, which can cause health hazards in urban areas.<sup>2</sup> Recent focus on sustainability and alternative energy resources has led to an increasing trend in research and development of new energy devices. Fuel cells

<sup>a</sup>University of Maribor, Faculty of Mechanical Engineering, Institute of Engineering Materials and Design, Smetanova ulica 17, 2000 Maribor, Slovenia. E-mail: selestina.gorgieva@um.si; Fax: +386 2 220 7990; Tel: +386 2 220 7935

<sup>b</sup>Dravske elektrarne Maribor d. o. o., Obrežna ulica 170, 2000 Maribor, Slovenia

<sup>c</sup>University of Maribor, Faculty of Electrical Engineering and Computer Science, Institute of Automation, Koroška cesta 46, 2000 Maribor, Slovenia

<sup>d</sup>Graz University of Technology, Institute for Chemistry and Technology of Biobased Systems, Stremayrgasse 9, 8010 Graz, Austria



Maša Hren obtained her master's degree in chemical engineering in 2018 and is currently pursuing a PhD degree at the Faculty of Mechanical Engineering, University of Maribor where she is focusing on the field of (bio)polymer chemistry. Her research interests lie in the field of fuel cells with a special focus on biopolymer based anion exchange membranes (AEMs) and modification of

fillers (cellulose based) for improved AEM properties.



Dr Mojca Božič received her PhD in Technical environmental protection from University of Maribor in Slovenia. She worked for 15 years at Faculty of Mechanical Engineering at University of Maribor, where she focused in the field of polymer biochemistry (expertise in enzymatic synthesis and biocatalysis, development of multifunctional biodegradable materials etc.) as an Assistant

Professor. Now she is working as a Project Manager at Dravske elektrarne Maribor d. o. o. and her research focus are renewable energy resources and circular economy.



are one of the most promising clean and efficient energy production technologies that convert chemical energy stored in fuels directly to electric energy and heat.<sup>3</sup> They use fuels containing hydrogen (including infrastructure hydrocarbon fuels such as ethanol, methanol, liquefied petroleum gas, *etc.*) and are often more efficient than internal combustion engines because they do not require an intermediate energy transformation into heat, and are, therefore, not limited by Carnot cycle efficiency.<sup>4,5</sup> Moreover, they provide electricity with zero emissions and high-energy conversion, and produce only water when hydrogen is used as the fuel. Fuel cells are composed mainly of solid parts, which makes them easier to produce and maintain, and the operation is silent, as they contain no moving parts. This makes them potentially highly reliable and long-lasting.<sup>5</sup>

Fuel cells that are currently under massive investigation include polymer exchange membrane fuel cells (*i.e.* proton exchange membrane fuel cells (PEMFCs) and anion exchange

membrane fuel cells (AEMFCs)), alkaline fuel cells, solid oxide fuel cells and molten carbonate fuel cells.<sup>6</sup> The general design of the mentioned fuel cells is similar, except for the electrolyte, which determines the operating temperature. PEMFCs have dominated commercially in vehicles to date (Toyota Mirai Fuel Cell Vehicle by Toyota Motor Co. in December of 2014),<sup>7</sup> but the supply of substantial quantities of hydrogen, the costs of establishing a supply infrastructure and the expense of systems have slowed market uptake.<sup>8</sup> On the contrary, the alkaline fuel cells, which, already in 1960, enjoyed considerable success in space applications for the Apollo space vehicle, have not been developed on a large-scale to date because of their electrolyte sensitivity to CO<sub>2</sub>.<sup>9</sup> They utilised an aqueous solution of KOH as a cheap electrolyte. The adoption of anion exchange membranes (AEMs) offers undoubtedly more advantages compared to a liquid electrolyte. Today, AEMFCs receive ever-increasing attention, because of their overwhelming superiority in comparison to PEMFCs: quicker electrochemical kinetics, lower catalysts cost and weaker corrosion.<sup>10</sup> In comparison to PEMFCs, the alkaline medium rendered by AEMFCs provides the potential to use non-precious-metal catalysts, which can facilitate commercialisation. Technically, AEMFCs are similar to PEMFCs, with the main difference being the solid AEM instead of an acidic PEM in PEMFCs.

As shown in Fig. 1, the number of peer-reviewed published articles on membranes for AEMFCs' applications has increased continuously over the last decade. This trend illustrates that the opportunity of designing new AEMs as promising candidates for AEMFC applications has attracted attention. The number of peer-reviewed articles has increased continuously, not only because of the introduction of emerging inorganic materials, but also due to advances in the preparation techniques for AEMs. Nevertheless, the number of scientists working on AEM materials is still very low, with communities dispersed across



*Prof. Dr Darinka Fakin obtained her PhD degree in 2004 from the Faculty of Mechanical Engineering, Institute of the Engineering Materials and Design, University of Maribor (FS-UM), Slovenia. She has more than 15 years of direct industrial praxis in textile industry (from technologies up to general director) and 20 years of research experiences in the field of textile chemistry with expertise in chemical functionalization of textile materials, today she works as a full professor at Faculty of Mechanical Engineering at the University of Maribor.*

*functionalization of textile materials, today she works as a full professor at Faculty of Mechanical Engineering at the University of Maribor.*



*Prof. Dr Karin Stana Kleinschek obtained her PhD degree in 1996 from the Institute of Physical Chemistry, University of Graz, Austria. Since 2007 she works as a full professor at Faculty of Mechanical Engineering at the University of Maribor (UM) and 15 years as Head of the Institute of the Engineering Materials and Design and the Laboratory for Processing and Characterization of Polymers at UM, Slovenia. At*

*the moment she is a full Prof at Faculty of Electrical Engineering and Computer Science, UM Maribor and since 2019 full professor and head of the Institute of Chemistry and Technology of Biobased Systems (IBIOSYS) at Graz University of Technology, Austria.*



*Assist. Prof. Dr Selestina Gorgieva obtained her PhD degree in 2014 from the Faculty of Mechanical Engineering, University of Maribor (FS-UM), Slovenia. She is currently employed as Scientific Associate at FS-UM and at Faculty of Electrical Engineering and Computer Science, UM. She is a member of several associations (European Society for Biomaterials, European Poly-*

*saccharide Network of Excellence), Editorial Board member for Processes (MDPI), and Special issue guest editor in Processes, Hindawi, and Bioengineering International. Her research focus is on biomaterials, (bio)polymers, nanocellulose (CNF, CNC, BC) modification and processing into films and scaffolds for technical and biomedical applications.*



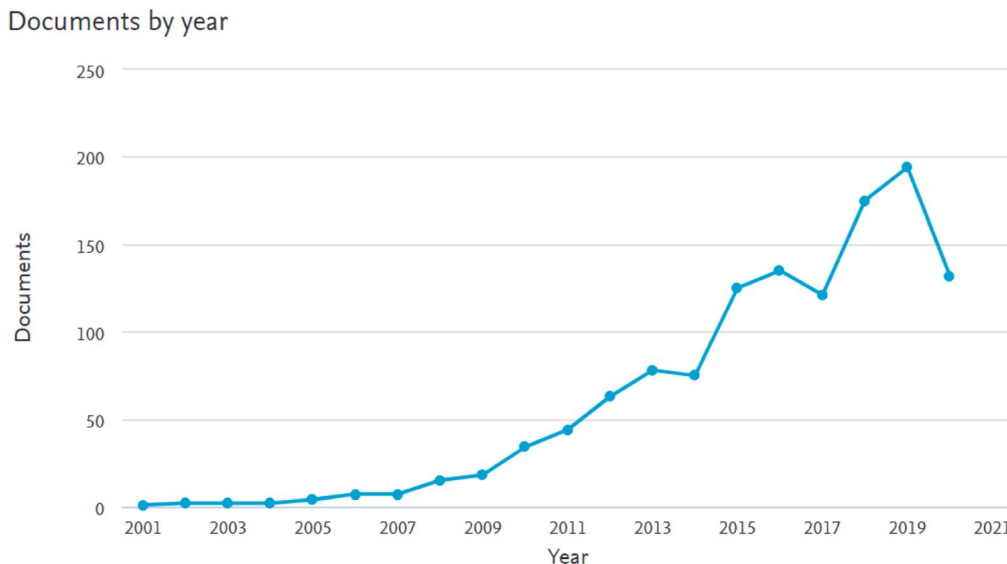


Fig. 1 Chronology of the advancement of anion conducting membranes for alkaline fuel cell applications. Source: <http://www.scopus.com>; search settings: anion exchange membranes (AEMs), alkaline fuel cells; excluded conferences, notes, books and review papers (accessed August 2020).

the world, with different regional strengths, technologies and challenges.

## 2. Anion exchange membrane fuel cells (AEMFC): components and materials

A single AEMFC includes the hardware (*i.e.* a gasket providing the seal around the membrane electrode assembly (MEA) to prevent leakage of gases) to protect the cell and the MEA. The latter consists of the AEM, the anode and cathode catalyst layers

and the cathode gas diffusion layer (GDL) (Fig. 2). The use of an AEM in the fuel cell creates an alkaline environment inside the cell. Common anion species crossing the membrane are the  $\text{OH}^-$ , generated according to the electrochemical oxygen reduction reaction (ORR) at the cathode. The  $\text{OH}^-$  are transported to the anode where the fuel (*e.g.*, hydrogen, methanol, ethanol *etc.*) in contact with electro-catalysts undergoes an oxidation reaction to generate a molecule of water per single electron. In AEMFCs, water is generated at the anode and, at the same time, water is a reactant at the cathode. The AEM should have the ability to allow the transport of  $\text{OH}^-$  ions while preventing fuel crossover and blocking the transport of electrons to prevent a circuit break.<sup>11–13</sup>

The anode and cathode GDL provides the main mechanical structure of the electrode, and provides support for the corresponding catalyst layer. The GDL acts as a transport channel for reactants and products which take part in the chemical reactions, and it also acts as an electric current collector and conductor, as well as a transporter of electrons to the current collector.<sup>12</sup> The GDL may be a porous structure of carbon fibre paper, a non-woven carbon fibre material (*i.e.* carbon felt, carbon foam), or a woven carbon fibre material with a micro porous layer (MPL) and hydrophobic treatment (*e.g.* polytetrafluoroethylene (PTFE)) to increase the surface contact with the membrane and to regulate water diffusion, respectively.<sup>15</sup> The MPL consists of carbon or graphite particles and 10–40 wt% of a hydrophobic binder, characterised by pore sizes of less than 500 nm compared to the substrate pores of more than 10  $\mu\text{m}$ .<sup>16</sup> The MPL-GDL design should be coupled tightly to the catalyst layer transport properties,<sup>17</sup> as if the same is hydrophilic and carries low water capacity (thin), then it is more prone to flooding, whereas a thicker catalyst layer can retain more water without flooding.<sup>7</sup>

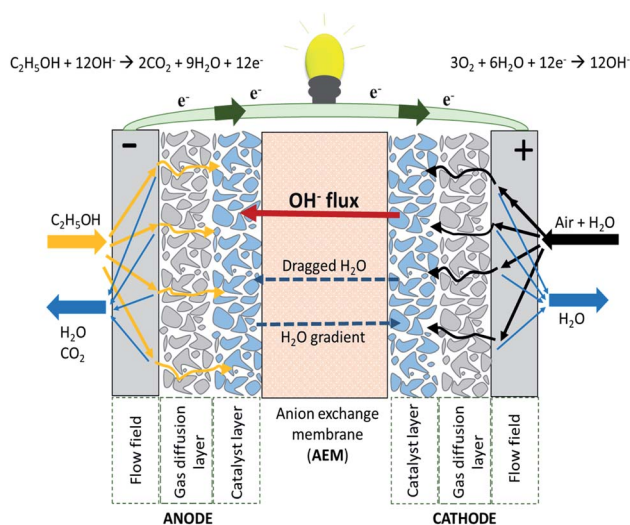


Fig. 2 Schematic representation of an alkaline anion exchange membrane fuel cell (AAEMFC) adapted from ref. 14 with permission from [Elsevier], copyright [2020].



The anode and cathode catalyst layers are positioned at the place where the chemical reactions, which produce electrical current, take place. They act as an active surface for the reactions, as well as a transport channel for reactants and products of chemical reactions.<sup>18</sup> AEMFCs are interesting systems because, among other advantages, non-Pt electro catalysts can be used, at either the anode, or the cathode, or both. In the case of hydrogen fuel, however, the non-Pt electro catalysts have been proven insufficient. The problem originates from the demand to maintain a partly oxide-free metal surface up to an anode potential of 0.1 V *versus* the reversible hydrogen electrode (RHE), and preferably higher, as required for the bonding of H<sub>ads</sub> intermediates in the relevant potential range.<sup>19</sup> Nonetheless, the clear advantage of the alkaline environment of an AEMFC stems from the fact that directly oxidising a complex fuel is practical, owing to the faster kinetics of many complex reactions in alkaline environments.

### 2.1. Fuel oxidation reaction at anode

Catalysts' selectivity towards the direct and complete oxidation of the fuel is desired, but these properties are difficult to achieve unless the reaction pathway is well understood. Anode catalysts differ from each other in terms of fuel type utilisation in alkaline conditions. The elimination of fuel reforming to produce hydrogen fuel in PEMFCs using liquid fuels (*i.e.* methanol, ethanol, hydrazine *etc.*) as a feed to the system makes AEMFCs an attractive option because of their simplicity. However, the selection of anode electrocatalysts that are suitable for individual fuel type is limited, and must be designed carefully. Especially, anode electrocatalysts that enhance individual fuel oxidation activity and minimise CO poisoning, must be considered to improve AEMFCs' performance.

To date, Pt based composite catalysts are still the most active metal for the hydrogen oxidation reaction (HOR).<sup>20</sup> In order to fulfil the potential of AEMFCs, anode as well as cathode catalysts should, in the near future, be free of Pt-based materials, and, eventually, free of critical raw materials. Novel materials must be designed whose intrinsic HOR activity is higher than presently reached with existing materials, and whose surface is not blocked for the HOR catalysis by the formation of oxide at a low overpotential.<sup>20</sup> Moving further in the group of Pt-based HOR catalysts, also investigated were the Ru/Pt core-shell nano catalysts with one or two Pt monolayers,<sup>21</sup> Au/Pt core-shell<sup>22</sup> and Pt/Cu nanowires.<sup>23</sup> Active non-Pt HOR catalysts reported for AEMFCs include Pd-based,<sup>24–28</sup> Ru-based,<sup>29</sup> Ir-based,<sup>30,31</sup> Rh-based<sup>32</sup> and Ni-based<sup>33–37</sup> materials. The addition of oxides like CeO<sub>2</sub>, NiO, Co<sub>3</sub>O<sub>4</sub> and Mn<sub>3</sub>O<sub>4</sub> can promote the activity and stability of Pd/C catalysts significantly.<sup>38</sup> However, in regards to the Pd-based catalysts, at the present ratio of market prices of Pd to Pt (>0.5) and considering the lower power densities achievable to date with Pd at relevant cell voltages, there is no economic advantage in replacing Pt by Pd as the AEMFC anode catalyst.<sup>19</sup>

A pure Pt catalyst is also the most active metal for the dissociative adsorption of methanol and ethanol. However, Pt is easily poisoned by the CO produced by methanol/ethanol

electro-oxidation at low temperatures. Alloying Pt with other metals, such as Ru, Mo, Sn, Re, Os, Rh, Pb and Bi, can improve the performance of a catalyst, as it gives tolerance to the poisoning species.<sup>38</sup> Given their relatively high activity in methanol/ethanol oxidation reactions, Pt based catalysts are suitable anode electro catalysts for AEMFCs. The kinetics of methanol/ethanol oxidation can improve significantly upon the addition of a second metal, such as Ru alloys with Pt.<sup>39</sup> The performance of AEMFCs can be improved by embedding Pt on metal oxides, such as RuO<sub>2</sub>, MnO<sub>2</sub>, MoO<sub>2</sub>, and IrO<sub>2</sub>.<sup>40,41</sup> Ni and Co are interesting metals for the alkaline electro oxidation of non-carbonaceous fuels (*i.e.* hydrazine), provided they are combined (sometimes alloyed) with co-elements that prevent their passivation, and enable directing the mechanism to the proper pathway.<sup>42–44</sup>

### 2.2. Oxygen reduction reaction (ORR) at cathode

Noble metals such as Pt and Pd are used commonly as primary catalysts for ORR.<sup>45–47</sup> New, kinetically better performing catalysts are being researched because the ORR on the cathode is kinetically sluggish.<sup>48</sup> To increase ORR performance, Pt and Pd were combined with other transition metals, such as Ru,<sup>49</sup> Sn,<sup>50</sup> Pb, Au,<sup>51</sup> Ni,<sup>52</sup> Ag,<sup>47,52</sup> Cu<sup>52</sup> or Co.<sup>52–54</sup> The intrinsically non-corrosive environment of AEMFCs allows the use of less noble electrocatalysts than Pt for ORR on the cathode side of MEAs. Therefore, also, materials from families of base metal oxides (MnO<sub>x</sub>, mixed oxides, spinels *etc.*),<sup>47</sup> M–N–Cs (M = Fe, Co, Mn *etc.*),<sup>48,55</sup> Ag<sup>46,47,56</sup> and Ni-based<sup>57</sup> materials have been studied extensively as ORR catalysts in alkaline media. The ORR activity of some pyrolysed Fe–N–C catalysts is now comparable to, or even higher than, that of Pt-based catalysts in basic media.<sup>20</sup> A B,N-codoped Cu–N/B–C nanomaterial was prepared as an ORR catalyst in alkaline electrolytes, which demonstrated superior stability and higher tolerance to methanol crossover in comparison to Pt/C catalyst, and was also shown to have suitable properties for use in an AEMFC.<sup>58</sup>

Microstructure and the fabricating method of electrodes associated with their transport resistances and electrochemical kinetics are critical for the improvement of cell performance. Modern AEMFC electrocatalyst layers are usually composite structures of anion conducting ionomer material and noble or non-noble metal catalyst, usually supported on carbon.<sup>59</sup> The characteristics of a good catalyst support material include the presence of surface functional groups that support catalyst-support interaction, a mesoporous structure that improves the triple phase boundary, electrochemical stability, high electrical conductivity, a high surface area and corrosion resistance. The use of carbon-based support with various structural and morphological properties improves the stability and electro catalytic activity of the catalyst. With the use of carbon support, mass transfer and electronic conductivity in the catalyst layer are found to be enhanced.<sup>60</sup> Conventionally, a carbon material such as carbon paper and carbon cloth is used as an electrode supporting substrate for the AEM, as well as carbon nanofibres, ordered mesoporous carbons, carbon aerogels, carbon nanohorns, carbon nanocoils, carbon nanotubes, multiwall carbon



nanotubes, graphite and graphene.<sup>60,61</sup> Especially, carbon paper and carbon cloth materials possess the merit of low-cost and high electronic conductivity. However, they have no promotion on the catalytic activity for electrode reactions. Therefore, various novel catalyst support materials, such as protonated polyaniline coated tungsten carbide nano composite, nitrogen doped graphene, sulfurized carbon xerogels, mesoporous structured hollow graphitised carbon spheres, have been used as Pt support.<sup>60</sup> Inorganic metal oxides have been studied to determine whether they can serve as good catalyst supports. Replacing carbon with traditional metal oxides is difficult, as they have insulating properties at temperatures lower than 200 °C. Among other materials, stoichiometric metal oxides such as reduced oxidation state titania, doped metal oxides (doped TiO<sub>2</sub> and SnO<sub>2</sub>) and nanostructured metal oxides (such as TiO<sub>2</sub> nanotubes and WO<sub>3</sub> nanorods), as well as iridium oxide and silicon carbide, have been proposed for use as electrically conductive support materials with high corrosion resistant properties.<sup>61,62</sup> There are numerous factors that contribute to the high cost of a fuel cell stack; however, the price of platinum (Pt) and Pt alloys is one of the main contributors. Therefore, the development of highly efficient and low-cost catalysts for both anode and cathode is essential for lowering system costs in the future.

### 2.3. Anion exchange membranes (AEMs)

Membranes are the heart of the fuel cells. They play a prominent role on the transport properties within fuel cells through the following factors: (i) friction by the pore walls, (ii) the energetics of the membrane swelling process, (iii) complete blocking of transport with insufficient water uptake, (iv) hydrophobic/hydrophilic interactions with water dipoles and solvation shells, (v) double-layer effects, and (vi) surface diffusion (*i.e.*, surface hopping processes along the side chains in AEMs).<sup>63</sup>

These devices can work only if the ion exchange membranes separate the anode and the cathode chambers and mediate the conducting ions (*e.g.*, protons and hydroxide ions) for the electrochemical reactions in the system.<sup>64</sup> AEMs are usually solid polymer electrolytes, which consist of a hydrophobic polymer backbone with attached functional positively charged hydrated ions and surrounding water molecules.<sup>65</sup> The main

function of the alkaline AEMs is to transport OH<sup>-</sup> anions from the cathode to the anode, and, at the same time, to block electron and fuel crossover at high alkaline conditions. The ideal polymer for AEMs must have excellent OH<sup>-</sup> conductivity, chemical and thermal stability, strength, flexibility, low gas permeability, low water drag, low cost and good availability. Usually the implementation strategy for the anion conductive structure (Fig. 3b) is to design a hydrophobic side chain into the original structure of a membrane, where the cation, typically quaternary ammonium (-NR<sub>3</sub><sup>+</sup>), is attached closely onto the polymer backbone, and the anion (OH<sup>-</sup>) is dissociated in the aqueous phase. The membrane conducts anions based on interactions between the hydrophilic positively charged functional groups and the negatively charged OH<sup>-</sup> anions. When the hydrated ions and surrounding water molecules (ionic clusters) in the membrane are dispersed across a hydrophobic matrix (Fig. 3a), the ionic transportation is inhibited by the surrounding hydrophobic walls, although small ionic channels can be formed through the dynamic assembly of ionic clusters. The ionic clusters are aggregated by increasing the content of hydrophobic structures and, thus, generate bigger ionic clusters to facilitate the formation of interconnected ionic channels (Fig. 3b).<sup>66</sup>

**2.3.1. Synthetic AEMs.** A variety of synthetic polymers have been proposed for AEMs' processing by the paste method,<sup>67</sup> block polymerisation,<sup>68</sup> copolymerisation,<sup>69</sup> direct solution casting,<sup>70</sup> the sol-gel technique,<sup>71</sup> grafting and plasma polymerisation<sup>72,73</sup> and the pore-filling method.<sup>64,74</sup> They include: polyphenylene oxide (PPO), poly(ether ether ketone) (PEKK), poly(ether ether ketone ketone) (PEEKK), ethylene tetrafluoroethylene (ETFE), polyvinyl alcohol (PVA), polyethyleneimine (BPEI), polytetrafluoroethylene (PTFE), polybenzimidazole (PBI), poly(olefins), styrene, and many others. Such a material is then functionalised by various reagents to obtain a positively charged AEM, carrying functionalities presented on Fig. 4.

Early studies on synthetic AEMs dated from 1988,<sup>75</sup> when a patent was applied for an all alkali electrolyte fuel cell containing a fluorine series AEM. In 2000, a patent was applied for<sup>76</sup> novel graft polymeric membranes comprising one or more alpha, beta, beta-trifluorovinyl aromatic monomers of specified formulae, radiation graft polymerised to a polymeric base film to be used as ion exchange membranes. In 2002, Danks *et al.*<sup>77</sup> published their work on vinylbenzyl chloride radiation grafted

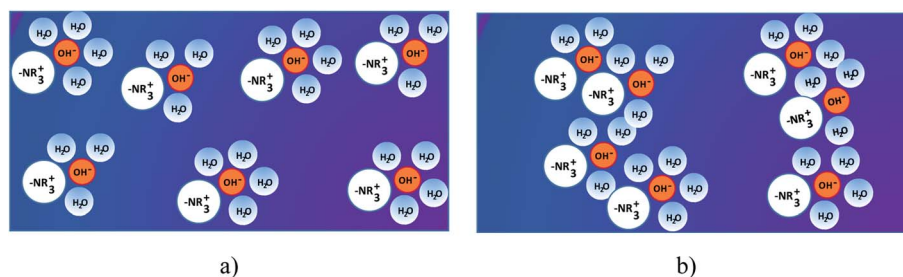


Fig. 3 Schematic representation of ionic pathways in an alkaline polymer membrane. (a) Ionic clusters are dispersed homogenously in the hydrophobic matrix (purple). (b) By introducing an additional hydrophobic structure, the ionic clusters aggregate, which facilitates the formation of interconnected ionic channels.



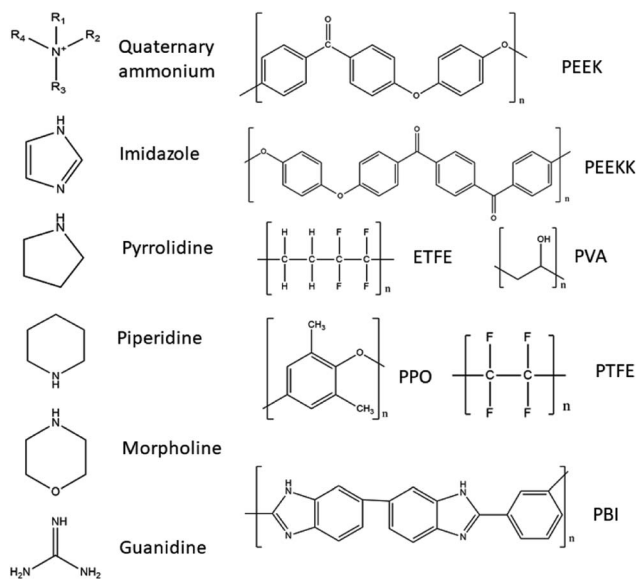


Fig. 4 Functional groups and synthetic backbones for AEMs.

onto both poly(vinylidene fluoride) and poly(tetrafluoroethylene-co-hexafluoropropylene) fluoropolymer films with subsequent amination, which formed AEMs suitable for use in low temperature direct methanol fuel cells (DMFC). In 2005, Li and Wang<sup>78</sup> prepared an AEM based on quaternised polyethersulfone through chloromethylation, quaternisation and hydrolytic reaction, which was also marked suitable for use in DMFCs. In 2006, Varcoe and Slade<sup>79</sup> reported a novel quaternary-ammonium-functionalised radiation-grafted poly(ethylene-co-tetrafluoroethylene).

In Table 1 several different AEMs suitable for use in DAFCs are listed, and classified regarding their backbone polymer material and the type of functional group present in the AEM. The main approach for enhancing the alkaline stability that has been studied is the individual cation approach with almost no focus on the synergetic effects between adjacent cations, in spite its effects on alkaline stability.<sup>80</sup> Therefore, the listed AEMs are mainly single cation type but studies have investigated multiple cation AEMs as well. It is believed that designing multi-cation side-chain type polymer AEMs is a good approach to obtain improved ion conductivity and enhance alkaline stability. It has also been demonstrated that AEMs with multi-cation side chains improve the conductivity due to large ionic clusters and microphase separation.<sup>80</sup> Also, the length of alkyl spacer (on the side chain) may influence ion conductivity and alkaline stability of the AEM.<sup>81</sup> It has been reported that grafting multiple cations on the polymer backbone can form hydrophilic/hydrophobic micro-phase separation and decrease the functional degree of the copolymer, which can restrain the degradation of the polymer backbone.<sup>82</sup> Studies of the relationship between the degree of functionalization and the structure of the side chain (in terms of charge number and charge arrangement) have been performed, notably on PPO-based AEMs with different kinds of quaternary ammonium side chains (triple, double and single-cation per cation side

chain) and have found that multiple cation AEMs exhibited a higher ionic conductivity and lower water uptake due to the phase separation of the hydrophobic domains at low degree of functionalization and larger ionic clusters induced by the presence of the side chains.<sup>83</sup> A study investigated the trade-off dilemma between ion conductivity and water uptake in poly(biphenyl alkylene)-based AEMs tethered with multiple quaternary ammonium groups per side chain. They prepared AEMs with similar IEC levels in order to allow direct comparison and multi-cation presence effects on the AEM's properties. They observed an increased phase separation and improved ion diffusion coefficient with increased amount of quaternary ammonium on the side chain as well as a much improved performance. However, such membranes have shown an inferior alkaline durability in comparison to AEMs with a low number of quaternary ammonium on the side chains.<sup>84</sup>

Several studies on cation backbone type AEMs have also been performed, including a study by Tan *et al.*<sup>80</sup> which have investigated main-chain polymers with pyrrolidinium cations tethered with different methylene groups. They conducted that increasing cation charge density of the pyrrolidinium compounds provided better alkaline stability, but a long spacer between the pyrrolidinium cations accelerated cations degradation in alkaline solutions. A synergetic effect between the adjacent pyrrolidinium cations lead to a lower charge density and improved alkaline stability. A new class of poly(arylene piperidinium)s have been synthesized by Olsson *et al.*,<sup>85</sup> which are a new class of aromatic cationic polymers for AEMs, containing quaternary piperidinium rings directly in the backbone, which are devoid of any weak benzylic hydrogens or aryl ether bond. Their study demonstrated that such membranes have a high alkaline stability and show high performance as long as the polymers are structurally designed to facilitate efficient strain relaxation. Olsson *et al.*<sup>86</sup> also prepared a series of AEMs based on poly(arylene piperidinium) with positive charge on the backbone with partial quaternization, copolymerization and *in situ* crosslinking with tuned IECs. Wang *et al.*<sup>87</sup> designed poly(aryl piperidinium) AEMs with adequate ionic conductivity, chemical stability and mechanical robustness due to the combination of the piperidinium cation and the rigid ether-bond free aryl backbone.

**2.3.2. Naturally derived membranes.** Synthesis of synthetic polymer AEMs is usually complex and time consuming, as well as environmentally unfriendly. Therefore, it is highly desired that the material is bio-renewable, non-toxic and environmentally benign.<sup>108</sup> Naturally derived materials are an alternative, where chitosan (CS), nanofibrillar cellulose (CNF) and nanocrystalline cellulose (CNC) have been, up to now, proposed as promising. CS is a cationic polymer, as it contains  $-NH_2$  groups which are positively charged in acidic media. This abundant polysaccharide of animal origin can readily form films, has a high mechanical and chemical stability and, on its own, is a weak alkaline polyelectrolyte.<sup>109,110</sup> It can be modified readily by attachment of different moieties (Fig. 5), which increases its positive charge. Currently, in spite of all the presented benefits, CS AEMs are still not advantageous in comparison to synthetic AEMs, especially in terms of ionic conductivity (up to now



Table 1 Synthetic AEMs, their backbones and functional groups

| Backbone                                     | Functional ionic group                 | Membrane   | Reference |
|--|--|--|-----------|
| Poly(ether ether ketone) (PEEK)              | Quaternary ammonium                    | AEMs based on one-step banylation modification of poly(ether ether ketone) (QBz-PEEK-x)  | 88        |
|  | Quaternary ammonium, imidazole         | TMD/ImPEEK AEM from chloromethylated poly(ether ether ketone) (CMPEEK), quaternised by <i>N,N,N,N</i> -tetramethyl-1,4-phenylenediamine (TMPD) and 1-methylimidazole | 89        |
| Poly(ether ether ketone ketone) (PEEKK)      | Imidazole                              | PEEKK-DImOH → imidazolium functionalised poly(ether ether ketone ketone) AEM   | 90        |
| Ethylene tetrafluoroethylene (ETFE)          | Quaternary ammonium                    | ETFE-based radiation grafted AEM with benzyltrimethylammonium head group (ETFE-TMA)  | 91        |
|  |  | Poly(trimethylaminostyrene hydroxide)-grafted poly(ethylene-co-tetrafluoroethylene (ETFE)) (An-AEM/OH)   | 92        |
|  | Pyrrolidine                            | ETFE-based radiation grafted AEM with benzyl- <i>N</i> -methylpyrrolidinium head-group (ETFE-MPY)  | 91        |
|  |  | ETFE- <i>g</i> -poly(vinylbenzyl- <i>N</i> -methylpyrrolidinium)-based AEM   | 93        |
|  | Piperidine                             | ETFE-based radiation grafted AEM with benzyl- <i>N</i> -methylpiperidinium head-group (ETFE-MPRD)  | 91        |
|  | Imidazolium                            | Polyvinylimidazolium hydroxide-grafted AEM (MNVIm/St-AEM (OH))   | 94        |
| Polyolefin                                   | Quaternary ammonium                    | AEM based on tetraalkylammonium-functionalised fluoropolyolefin (PBFB-QA)  | 95        |
|  |  | AEMs based on fluoropolyolefin with quaternary ammonium cationic groups  | 96        |
|  |  | Polyolefin-based AEMs with single or triple-cation per side chain  | 97        |
|  |  | Poly(2,6-dimethyl-1,4-phenylene oxide) grafted with tailored polystyrene chains (QAPPO- <i>g</i> -PS-x)  | 98        |
| Poly(2,6-dimethyl-1,4-phenylene oxide) (PPO) | Quaternary ammonium and other N groups | QA-PPO or poly(2,6-dimethyl-1,4-phenylene oxide)s (PPO) based AEM with ammonium headgroup  | 99        |
|  | Quaternary ammonium                    | Mono- and di-functionalised comb-shaped poly(2,6-dimethylphenylene oxide) based alkaline stable AEM for FC   | 100       |
|  | Imidazole                              | IM-PPO or poly(2,6-dimethyl-1,4-phenylene oxide)s (PPO) based AEM with imidazolium headgroup   | 99        |
|  |  | A flexible, hydrophilic side-chain type AEM with ethylene oxide spacers incorporated into imidazolium-containing cationic side-chains                                | 101       |
|  |  | AEM based on poly(phenylene oxide) (PPO) chains linked to pendant 1,2-dimethylimidazolium (Dim) functional groups  | 102       |





Table 1 (Contd.)

| Backbone  | Functional ionic group | Membrane  | Reference |
|---|------------------------|---|-----------|
|   | Piperidine             | PI-PPO or poly(2,6-dimethyl-1,4-phenylene oxide)s (PPO) based AEM with piperidinium headgroup   | 99        |
|   | Morpholine             | MO-PPO or poly(2,6-dimethyl-1,4-phenylene oxide)s (PPO) based AEM with morpholinium headgroup   | 99        |
| Polyvinyl alcohol (PVA) and branched polyethyleneimine (BPEI)         | Quaternary ammonium    | Polyvinyl alcohol/branched polyethyleneimine (PVA/BPEI) prepared with casting with glutaraldehyde quaternised with benzyl chloride  | 103       |
| Polyvinyl alcohol (PVA)   | Quaternary ammonium    | Organic-inorganic hybrid anion-exchange silica precursor with ammonium functionality by ring opening of glycidoxypropyltrimethyl ammonium   | 71        |
| Polytetrafluoroethylene (PTFE)  | Guanidinium            | Semi-interpenetrating bi-guanidinium polysilsequioxane composite membrane with PTFE   | 104       |
| Poly(arylene ether sulfone)   | Imidazole              | Poly(arylene ether sulfone) with bulky imidazole groups based on a novel monomer 2,2-bis-(2-ethyl-4-methyl-imidazole-1-ylmethyl)-biphenyl-4,4-diol (EMIPO)                          | 105       |
| Polybenzimidazole (PBI) and poly(vinylbenzyl chloride) (PVBC) (1 : 1) | Quaternary ammonium    | PBI-c-PVBC-OH-1 : 1 double cross-linked AEM based on PBI (polybenzimidazole) and (PVBC) poly(vinylbenzyl chloride) with <i>N,N,N,N</i> -tetramethyl-1,6-hexanediamine (quaterniser) | 106       |
| Styrene and acrylonitrile (1 : 3)                                     | Imidazole              | <i>In situ</i> cross-linked styrene, acrylonitrile, 1-methyl-3-(4-vinylbenzyl) imidazolium chloride   | 107       |
|   | Quaternary ammonium    | <i>In situ</i> cross-linked styrene, acrylonitrile, and <i>N,N,N</i> -trimethyl-1-(4-vinylphenyl) methanaminium chloride  | 107       |

reaching  $10^{-2} \text{ S cm}^{-1}$  (ref. 111)) and mechanical properties, where the latter can be improved by the introduction of fillers.

Table 2 summarises several different naturally derived AEMs suitable for use in DAFCs, where classification is made regarding their backbone polymer material and the type of functional group.

**Chitin and CS.** Chitin, otherwise known as (1,4)-*N*-acetyl-D-glucose-2-amine, is a natural polysaccharide of animal origin. The polymer is produced by a variety of living organisms, and is the second most abundant natural polymer in the world, right after cellulose. In nature, chitin occurs as one of the main components of exoskeletons of crustaceans and cell walls of fungi, where it is included in the protein matrix and has the ability to modify its properties. The most obvious such modification is the encrustation with calcium carbonate, which results in a stronger, more rigid structure of the exoskeleton. Although it is abundant, its main sources are the shells of crabs and shrimps ( $\alpha$ -chitin), as well as squid and prawns ( $\beta$ -chitin). Chitin is extracted from crustaceans with acid treatment, which

dissolves the calcium carbonate followed by alkaline extraction, which dissolves the proteins. This is usually followed by a process of discolouration, which removes the remaining pigments, leaving colourless chitin. The difference between chitin and CS lies in the degree of deacetylation, as they have a similar chemical structure with OH groups, with the difference in the C2-atom, where an  $-\text{NH}_2$  group is present in CS and acetamide group on chitin. The name CS is usually used when the degree of deacetylation reaches 70% or more. The deacetylation degree reaction in hot alkaline conditions usually reaches a maximum of 95%.<sup>140</sup>

CS is a derivative of chitin. It is a low-cost biopolymer with a positive charge ( $-\text{NH}_2$  groups in CS are responsible for the positive charge) in acidic media, although on its own it is a weak poly-electrolyte and has a high chemical and mechanical stability, coupled with an ability to form films readily.<sup>109,110</sup> CS's cationic character is unique, as it is the only pseudo-natural cationic polymer.<sup>140</sup> It has predominantly alkaline characteristics, caused by an abundance of  $-\text{NH}_2$  groups present in CS





Fig. 5 Functional groups and chitosan (CS) and cellulose backbones.

(6,2 mmol g<sup>-1</sup>), which can conduct OH<sup>-</sup> anions. In the dry state a cross-linked, unmodified CS membrane is almost non-conductive. Only after hydration does such a membrane showcase characteristics of ion-conductivity.<sup>117</sup>

**Nanocellulose.** Cellulose is the most abundant natural, biodegradable and bio-renewable material with low weight, low density, exceptional mechanical properties and functionalisation potential, as it contains many OH groups.<sup>141</sup> Different types of nanocellulose are differentiated by the production processes, and include nanocrystalline cellulose (CNC), nanofibrillar cellulose (CNF) and bacterial cellulose (BC), characterised by different morphology, particle size, crystallinity, *etc.* CNFs consist of long fibrils with a diameter between 1–100 nm and a length of 500–2000 nm, high surface area and interchanging crystalline and amorphous regions.<sup>142</sup> BC has an identical molecular structure to CNFs and it is free of the lignin, hemicellulose and pectin found in its plant relatives.<sup>143,144</sup> It also possesses distinguishing features such as ultra-high crystallinity (up to 90%), polymerisation degree, a large surface area and remarkable mechanical properties in terms of flexibility and tensile strength. It is produced from various Gram, non-pathogenic bacterial strains.<sup>144</sup>

**2.3.3. Modification and cross-linking.** CS possesses the ability of chemical modification due to the presence of –NH<sub>2</sub> and –OH groups on the polymer backbone.<sup>110</sup> Several different approaches have been investigated for the modification of CS. Some of them are quaternisation with glycidyl trimethyl ammonium chloride (GTMAC),<sup>145</sup> 2-hydroxypropyltrimethyl ammonium chloride (CHPTAC),<sup>146</sup> benzyltrimethylammonium chloride (BTMAC),<sup>70</sup> iodomethane,<sup>147</sup> betaine in the presence of coupling reagent 2-ethoxy-1-ethoxycarbonyl-1,2-dihydroquinoline (EEDQ),<sup>148</sup> 2-[(acryloyloxy)ethyl]trimethylammonium chloride (AETMAC),<sup>149</sup> pyridine carboxaldehyde in combination with iodomethane.<sup>150</sup> The –OH group present on cellulose also offers abundant opportunities for modification, such as with the green chemistry approach of cationic quaternisation with a cholin based ionic liquid.<sup>151</sup>

Polymer crosslinking has been used in order to prepare durable AEMs with improved mechanical and chemical stability.<sup>110</sup> Different substances have been used as covalent cross-linkers for synthetic, natural or composite membranes, including glutaraldehyde<sup>111,113,115,117,135,146</sup> ethylene glycol diglycidyl ether,<sup>117,135</sup> epichlorohydrin<sup>113</sup> trimethylolpropane triglycidyl ether<sup>152</sup> and a green reagent genipin,<sup>153</sup> which were all used for the crosslinking of CS (Fig. 6a). As tentatively presented in Fig. 6b, crosslinking of CS with glutaraldehyde involve reaction of the aldehyde groups present in glutaraldehyde with the –NH<sub>2</sub> groups on CS, forming Schiff's bases. The epoxide groups present on epichlorohydrin, trimethylolpropane triglycidyl ether and ethylene glycol diglycidyl ether react mainly with –OH groups on CS and undergo a cleavage of the epoxide ring and condensation reaction, making it also usable for other polysaccharides.<sup>152</sup> In the case of genipin, reactions have been reported between the –NH<sub>2</sub> groups on CS, proceeding through different mechanisms.<sup>154</sup>

**2.3.4. Membrane properties.** In an MEA the membrane is constrained between the electrodes; therefore, an important factor on the membrane-electrode interfacial resistance is membrane swelling, which may lead to electrode delamination. Swelling, as well as contraction of the membrane in a MEA, can cause pinhole and crack formations due to the accumulated hydrothermal stress experienced by the membrane.<sup>155</sup> Other factors with a lesser impact include the mismatch of electro-osmotic drag coefficients of the membrane and electrodes, and poor adhesion between dissimilar polymers.<sup>156</sup>

**Ionic conductivity and OH<sup>-</sup> ions' transport.** Ionic conductivity in AEMs is an important parameter in AAEMFCs, and the same depends on the concentration and the mobility of OH<sup>-</sup> anions through the membrane, and is also related to the membrane's transport properties.<sup>64</sup> High anion conductivity has a positive effect on the power density, and is responsible for lower power/ohmic losses.<sup>65</sup>

Ionic conductivities of AEMs are generally lower than those of PEMs.<sup>157</sup> The reason for this lies mainly in the lower mobility of the hydroxide ion in comparison to proton but also in the



Table 2 Naturally derived AEMs: respective backbone and functional groups

| Backbone   | Functional ionic group                           | Membrane   | Reference  |  |
|--|--|--|--|--|
| Chitosan (CS)  | None added                                       | CS membrane  | 112  |  |
|  |  | Glutaraldehyde cross-linked CS   | 113  |  |
|  |  | Three-layered CS loaded with KOH cross-linked with glutaraldehyde  | 114–116  |  |
|  | Quaternary ammonium                              | Glutaraldehyde cross-linked quaternised CS   | 111  |  |
|  |  | Quaternised CS derivatives cross-linked with ethylene glycol diglycidyl ether  | 117  |  |
|  |  | Cross-linked quaternised CS with tetraethoxysilanes  | 118  |  |
|  |  | CS modified with polymeric reactive dyes   | 119  |  |
|  |  | CS membrane modified with a reactive cationic dye  | 120  |  |
|  |  | Composite of CS, ionised organic compound and hydroxylated multiwalled carbon nanotubes cross-linked with glutaraldehyde | 121  |  |
|  | Quaternary ammonium and other ammonium compounds | Imidazolium functionalised brushes   | Functionalised MXene embedded into a CS matrix   | 122  |
|  |  |  | Added ionic liquid   | Mixed matrix based on CS and fillers (ionic liquid IL, metallic Sn powder, layered titanosilicate, layered nanosilicate) |
|  | Quaternary phosphonium K <sup>+</sup> crown ion  | Phosphoryl group   | Composite membrane from quaternary phosphonium polymer microsphere incorporated into CS  | 124  |
|  |  |  | CS grafted diformyl-dibenz-18-crown-6 with added K <sup>+</sup> on the crown ion         | 125  |
|  |  |  | Phosphorylated CS AEM  | 126  |
|  | CS and polystyrene (PS) composite                | Quaternary ammonium  | AEM with a semi-interpenetrating polymer network based on quaternised CS and polystyrene | 127  |
| Quaternary ammonium and fillers with positive charge                 |  | Quaternised CS and positively charged polystyrene cross-linked with glutaraldehyde                                       | 128  |  |
| CS, PS and polyacrylamide CS and poly(vinyl alcohol) (PVA) composite | Quaternary ammonium                              | Full interpenetrating network from quaternised CS, polyacrylamide and polystyrene  | 129  |  |
|  | Quaternary ammonium                              | Quaternised PVA and quaternised CS cross-linked with glutaraldehyde  | 130  |  |
|  |  | PVA and quaternised CS cross-linked with glutaraldehyde  | 131  |  |
|  |  | Composite of quaternised PVA and quaternised CS nano particles   | 132  |  |
|  |  | Quaternised PVA/CS/molybdenum disulfide AEM  | 133  |  |
|  |  | CS nanoparticles incorporated into quaternised PVA   | 134  |  |
|  |  | Cross-linked quaternised CS and quaternised PVA by ethylene glycol diglycidyl ether                                      | 135  |  |
|  |  | Cross-linked quaternised CS and quaternised PVA by glutaraldehyde  | 135  |  |
| None added   | None added                                       | Cross-linked PVA/CS solution casting or electrospun nanofibre  | 136  |  |
|  |  | PVA/CS nanocomposite membrane with graphene (graphene or sulfonated graphene)  | 137  |  |
| CS and tetrabutyl titanate   | Quaternary ammonium                              | Organic–inorganic hybrid: cross-linked quaternised CS with tetrabutyl titanate   | 138  |  |
| Cellulose nanocrystals (CNC) and polyphenylene oxide (PPO)           | Quaternary ammonium                              | Composite from quaternised CNC and quaternised PPO   | 139  |  |

insufficient dissociation and solvation of the hydroxide ion.<sup>158</sup> Most AEM membranes rely on quaternary ammonium functional groups as the bearers of a positive charge. These functional groups are less dissociated than the sulfonic acid group, which is the main functional group carrying negative charge in PEMs. This is expressed through  $pK_a$  values, as the  $pK_a$  for sulfonic acid groups is  $-1$ , and for quaternary ammonium groups it is  $4$ . Other reasons are morphology of the structure, influence of the structure on inhibiting transport mechanisms and interactions between  $OH^-$  anions and quaternary ammonium functional groups on the side chains in solution (in this

case, the anion conductivity can decrease because of  $CO_3^{2-}/HCO_3^-$  formation in the presence of air during the measurement).<sup>65</sup> The lower ionic conductivity of AEMs *versus* PEMs can also be attributed to the fact that PEMs consist of a hydrophobic matrix and of interconnected hydrophilic ionic channels or clusters, which means they have well-defined phase morphology. Because the synthesis process of AEMs does not lead to micro-phase separation phenomena, AEMs have a lower ionic conductivity.<sup>64</sup> The  $H^+$  ion diffuses through the PEM membrane more rapidly than the  $OH^-$  ion in an AEM. To overcome the problem of limited  $OH^-$  conductivity in AEMs the



research focused onto the development of new polymer chemistries (backbone and functional groups) in order to increase the anion conductivity.<sup>14</sup>

The amount of knowledge on the OH<sup>-</sup> anion transport mechanisms in AEMs is not as high as the knowledge about H<sup>+</sup> transport in PEMs. It is assumed that the same possible transport mechanisms occur in an AEM membrane as in a PEM membrane, as they observed similar trends in dependence on the transport coefficient (connected with conductivity) on humidity, pressure and the temperature by experiments.<sup>65</sup> The transport of OH<sup>-</sup> can be described with several transport mechanisms, which are listed below. Water molecules have an important role in the Grotthuss and diffusion transport mechanisms of OH<sup>-</sup> anions' transportation through the membrane. Water clusters have an important influence on the transport of OH<sup>-</sup> anions through the AEM, which means that an appropriate increase in the adsorption of water can improve the ionic conductivity through the membrane, yet a substantial increase in the adsorption of water can have a negative impact on the effectiveness of the membrane.<sup>121</sup>

*The Grotthuss mechanism.* The Grotthuss mechanism is considered as the main transport mechanism for the transport of OH<sup>-</sup> anions through AEM membranes. Also, in the case of a PEM membrane, this mechanism is considered as the main mechanism for the transport of H<sup>+</sup> ions. This mechanism is because both OH<sup>-</sup> and H<sup>+</sup> ions exhibit "grotto behaviour" in aqueous solutions. Grotto behaviour is defined as the hopping of H<sup>+</sup> ions through a series of water molecules interconnected by hydrogen bonds. A simplified explanation for the Grotthuss mechanism for OH<sup>-</sup> anions is diffusion of OH<sup>-</sup> anions through a network of water molecules interconnected by hydrogen bonds by the formation or cleavage of covalent bonds.<sup>65</sup> It is assumed that the movement of hydrated OH<sup>-</sup> anions is accompanied by a hyper-coordinated water molecule, which is the donor of the fourth hydrogen bond. The presence of an extra electron-donor water molecule leads to a rearrangement and reorientation of hydrogen bonds, as well as an H<sup>+</sup> ion transfer, which leads to the formation of a completely tetrahedrally coordinated water molecule.<sup>11</sup>

*The diffusion and/or migration.* The diffusion and/or migration of OH<sup>-</sup> anions is induced by the concentration and/or electro-potential gradient.<sup>11</sup> The diffusion in an AEM membrane occurs in the following manner: in aqueous solutions OH<sup>-</sup> anions combine with one or more water molecules (OH<sup>-</sup>(H<sub>2</sub>O)<sub>x</sub>) and travel through the membrane due to electro-osmotic drag. Such a mechanism occurs when there is free volume available within the polymer chains.<sup>65</sup>

*Convection.* Convection transport occurs due to the OH<sup>-</sup> anions migrating through the membranes, and, as they move, they drag water molecules with them through the membrane. By this they cause a convection flow of water molecules within the membrane.<sup>11</sup> The convection transport of OH<sup>-</sup> anions through an AEM membrane is caused by the pressure gradient.<sup>65</sup>

*Surface site hopping.* Surface site hopping is defined as the "hopping" of anions/cations from one cation/anion group to the

other in the presence of water, which acts as a permanent dipole. An OH<sup>-</sup> anion "hops" from one cation group on the surface of the membrane to the other through the AEM.<sup>65</sup> The surface site hopping of OH<sup>-</sup> anions takes place on quaternary ammonium groups, which are linked on the membrane. Such a transport mean is considered of secondary importance, as the water in an aqueous system acts as a permanent dipole, and interactions occur between the fixed positive quaternary ammonium groups on the membrane and water. These interactions lead to an orientation of water molecules around the cationic quaternary ammonium groups, which leads to a decreased possibility of interactions between the OH<sup>-</sup> anions and the cationic groups on the membrane.<sup>11,65</sup>

Obtaining accurate measurements of the hydroxide conductivity of AEMs is a significant challenge. There are issues with hydroxide exchange films: (i) the OH<sup>-</sup> anions in a membrane will react completely with the atmospheric CO<sub>2</sub> within 10 minutes of exposure to air, (ii) the cationic groups may not survive the presence of hydroxide, and may decompose when they are exchanged to the hydroxide form, or may decompose during measurement at higher temperatures. For the reliability of reported numbers obtained by measurements, films need to be checked for decomposition before and after testing. The AEM needs to be exchanged to the hydroxide form, and then washed thoroughly with degassed distilled water in the absence of CO<sub>2</sub>. The ionic conductivity should then be measured on an AEM prepared in such a way without CO<sub>2</sub>, with the use of high purity blanket gases and degassed water for humidification control.<sup>159</sup>

The ion conductivity measurements usually include: (i) pre-treatment of the samples, (ii) testing of membrane impedance and (iii) calculation of ionic conductivity from the data obtained by impedance.<sup>88</sup> The aim of the pre-treatment of AEMs is ion exchange, and it includes the conversion of AEM samples to the OH<sup>-</sup> or Cl<sup>-</sup> forms. In order to do so, the AEM samples are soaked in NaOH (different molarities and different durations have been found in the literature). After the ion exchange, the AEM samples are rinsed thoroughly with deionised water in order to remove any residual OH<sup>-</sup> or Cl<sup>-</sup> ions.<sup>101</sup> The standard method for the measurement of ion conductivity is impedance spectroscopy, which is carried out on the AEM samples after the pre-treatment. A two-point probe,<sup>95</sup> or four-point probe<sup>92,94,101</sup> alternating (AC) impedance spectroscopy technique can be used. Usually measurements are made in the longitudinal direction. Conductivity was measured under fully hydrated conditions in a beaker filled with N<sub>2</sub> saturated deionised water under specific temperature (60 °C in many articles).<sup>92,94</sup> The cell is also immersed in water, which was previously degassed and blanketed with flowing Ar to avoid carbonation and preserve the OH<sup>-</sup> form of the samples.<sup>95,98</sup> Some research groups also placed the testing assembly into an oven with controlled temperature and humidity to minimise errors due to the effect of CO<sub>2</sub> interferences.<sup>101</sup> The impedance was measured over a broad frequency range (from 1 MHz to 100 Hz,<sup>88,101</sup> 100 mHz to 100 kHz,<sup>95,98</sup> 100 kHz (ref. 92, 94 and 160)). The ionic conductivity was then calculated from the obtained data. Also a new, highly reproducible and improved way of measuring the conductivity



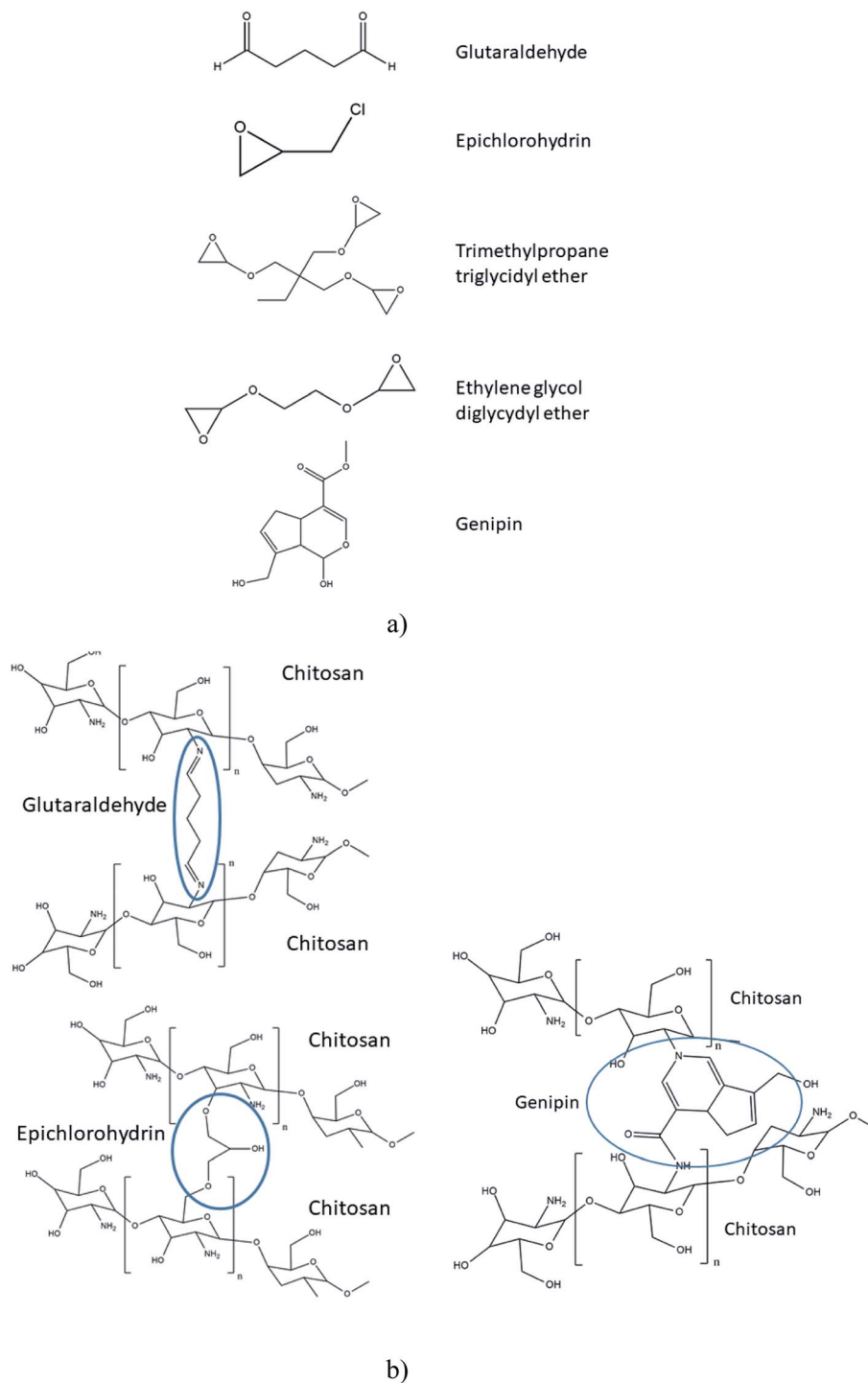


Fig. 6 (a) Cross-linked CS and (b) common cross-linkers suitable for CS crosslinking.

that does not involve chemical steps to convert the membrane into OH form has been described by Ziv and Dekel.<sup>161</sup>

**Ion exchange capacity (IEC).** In ideal conditions, when the membrane is not swollen, the conductivity of the membrane increases linearly with the increasing of IEC and is independent of the nature of the polymer. IEC is also linked to the water content in the membrane, therefore, at high IECs which yield increased water uptake, the ionic conductivity starts to decrease due to swelling and ionic dilution.<sup>83</sup> IEC is usually determined

with the titration of fixed functional ionic groups, like  $-R_4N^+$ , which are tethered to the membrane's polymer backbone. It is defined as the mol of cation groups present on the membrane (the functional groups taking part in the ion exchange) per mass unit of dry polymer membrane ( $\text{meq g}^{-1}$  dry membrane). If the fixed functional charged groups are monovalent the IEC is usually expressed as  $\text{mmol g}^{-1}$ .<sup>11,162</sup> Potentiometric, titration and spectrophotometric methods are mainly used for the IEC. The potentiometric method is based on measuring the change



in pH due to increased  $\text{OH}^-$  concentration in the solution, the titration method is based on titration of a membrane sample with  $\text{AgNO}_3$  to determine exchanged  $\text{Cl}^-$  and  $\text{NO}_3^-$  ions, and the spectrophotometric detection method is based on  $\text{NO}_3^-$  ions exchanged with  $\text{Cl}^-$  ions in the sample membrane.<sup>163</sup>

**Fuel crossover.** Fuel crossover is a serious challenge which fuel cells need to overcome in order to become commercially viable. Fuel crossover is defined as the permeation of fuel from the anode through the electrolyte AEM to the cathode.<sup>18,164</sup> The fuel crossover in an AEM occurs in the opposite direction than the flow of  $\text{OH}^-$  anions through the membrane, which means that the amount of fuel crossover is lower in an AEM than in a PEM, where fuel and  $\text{H}^+$  ions flow through the membrane in the same direction.<sup>65</sup> The main driving forces of fuel crossover are the concentration difference between the electrodes and electroosmotic drag. Electroosmotic drag contributes greatly to the fuel crossover in a PEM, but not in an AEM, where the effect is substantially reduced due to the opposite directions of fuel crossover and the flow of  $\text{OH}^-$  anions through the membrane.<sup>164</sup> Ethanol crossover in an AEM is lower due to the reversed electroosmotic drag of the hydrated  $\text{OH}^-$  anions in comparison with  $\text{H}^+$  conduction in a PEM.<sup>65</sup> The concentration difference in the fuel between the anode and cathode causes the fuel molecules to diffuse through the AEM membrane from the anode to the cathode.<sup>164</sup>

The fuel crossover rate depends on: (i) the type of fuel being used, (ii) the concentration of the feed fuel and (iii) operating conditions of the fuel cell. The feed concentration of fuel decreases if the fuel crossover is too high, which decreases the performance of the fuel cell due to limitations in mass transport at the anode. In addition, the fuel crossover is also increased if the feed concentration is too high. For these reasons the optimal concentration of the fuel feed needs to be determined for the specific conditions in which the fuel cell operates. The negative effects of fuel crossover include the reduction in cathode potential and cathode depolarisation. Therefore, fuel is wasted, and the overall efficiency of the fuel cell is reduced. The permeated fuel could possibly poison the cathode catalyst and the corresponding oxidation intermediate products.<sup>18</sup> Consequences of fuel crossover can include the (i) reduction in fuel utilisation, (ii) degradation of cathode activity, (iii) generation of extra heat, (iv) a decrease in the cell potential and (v) a reduction of the overall performance of the fuel cell. Some possible solutions for fuel crossover include dilution of the fuel, the use of a less permeable membrane to the chosen fuel and the development of a proper catalyst.<sup>164</sup>

**Durability and stability.** Increasing the durability of solid polymer electrolyte membranes applicable in fuel cells is necessary, particularly for AEMs where thinner films are needed. Membrane strength and durability can be influenced by different design factors. AEMs have lower transport efficiencies than PEMs, so the membranes need to be as thin as possible in order to minimise area specific resistance, therefore, maintaining mechanical integrity of the thin AEMs is difficult.<sup>155</sup> An ultra-thin membrane enables low ohmic resistance of the AEMs, and leads to a higher anion conductivity and a reduction of voltage losses in the fuel cell. Therefore, the membrane needs to be as thin as possible, and only as thick as

it is needed to guarantee mechanical stability under the fuel cell's operating conditions.<sup>65</sup>

**Mechanical properties.** Fuel cell lifetime is often determined by the ability of the membrane to withstand mechanical degradation. Mechanical degradation of an AEM occurs due to the combined physical and chemical stresses present in the fuel cell.<sup>155</sup> Basic mechanical properties are attributed mainly to polymer chemistry. Mechanical stability of an AEM depends mainly on the polymer backbone; increasing the concentration of ion exchange groups leads to a decrease in mechanical stability due to membrane swelling caused by excessive water uptake, or by membrane embrittlement because of dehydration. For this reason, the optimal amount of ion exchange groups needs to be determined, and should not be exceeded.<sup>65</sup>

When a block copolymer is used in an AEM, the mechanical properties can be tailored by selecting the right polymer chemistry of the hydrophobic block in order to achieve the desired properties. A common technique used in order to improve membrane strength is chemical crosslinking, which increases the Young's modulus and strength; however, it may reduce the ionic concentration and may cause membrane embrittlement. It has been shown that a higher degree of crystallinity can improve mechanical properties. This can be achieved by altering the polymer chemistry, such as reducing the length of side chains, or with various annealing techniques. It is also possible to reinforce the membranes physically with a nonconductive, porous, alkaline stable polymer film, which improves the durability. The reinforcement of an AEM also helps resist dimensional swelling, increases stability between dry and hydrated states and prolongs the lifetime of the AEM. The inclusion of a physical reinforcement can strengthen the AEM and resist changes in hydration, but the inclusion of a nonconductive material can be a drawback, as it lowers the ion exchange capacity of the AEM.<sup>155</sup>

Mechanical properties are characterised mainly by tensile strength tests, as well as *ex situ* durability tests, including rapid humidity cycling while monitoring gas crossover, pressurised blister tests, and mechanical fatigue testing by dynamic mechanical analysis, which have been shown to predict relative membrane lifetimes accurately.<sup>155</sup> A standard method ASTM D-1708 can be used for the measurement of mechanical properties, including tensile strength (MPa), Young's modulus (MPa) and elongation at break (%).<sup>95</sup> Membranes are immersed in deionised water, or heated at a certain temperature for 24 hours to obtain fully saturated or fully dry samples, respectively. Then the mechanical properties are measured. Measurements can be obtained by an electronic tensile tester or by dynamic thermomechanical analysis.<sup>101</sup>

**Thermal properties.** The thermal stability of an AEM depends greatly on the polymer backbone of the AEM.<sup>65</sup> Fuel cells could be applied in portable electronic devices, and they should operate at temperatures below 60 °C. Operating an AAEMFC at elevated temperatures, however, does have benefits, as it reduces thermodynamic voltage losses due to differences in pH across the AEM, and also improves electrokinetics.<sup>165</sup> Thermal stability can be determined by the thermogravimetry/differential scanning calorimetry (TGA/DSC),<sup>65</sup> usually carried out under  $\text{N}_2$  flow with a 10 °C  $\text{min}^{-1}$  heating rate. In such an analysis, the weight remaining as a function of temperature is recorded,<sup>92,98,101,103</sup> with temperature span up to 900 °C. Also,



thermogravimetric analysis-mass spectroscopy can be conducted under an He atmosphere.<sup>92</sup>

**Water uptake.** AEMs and PEMs require water for normal operation, as an optimal degree of hydration needs to be maintained in order to obtain optimal performance of the membrane. A membrane's water uptake depends on (i) the temperature, (ii) the dissociation constant and the number of conducting groups, (iii) the type of counter ions, (iv) the elasticity of the polymer matrix, (v) the hydrophobicity of the polymer surface and (vi) the pre-treatment of the membrane.<sup>18</sup> High water uptake can lead to membrane swelling, which leads to the degradation of mechanical and chemical properties of the membrane.<sup>64</sup> In an AEM, water is transported electro-osmotically from the cathode to the anode (the reverse of a PEM).<sup>165</sup> Fuel cells with AEMs exhibit more simplified water management than fuel cells with PEMs, since in the AEM, water is produced at the anode and consumed at the cathode (as opposed to PEMs).<sup>65</sup> In a PEM, flooding of the membrane is caused by electroosmosis of water from the anode to the cathode, because, in an AEM, the direction of electroosmosis is the opposite, as in a PEM, flooding is averted and mass transport-derived voltage losses are reduced.<sup>165</sup> The majority of water in an AAEMFC is produced with the reaction on the cathode, but water can also be introduced into the fuel cell if a diluted fuel is used.<sup>18</sup>

The conductivity of the membrane is enhanced with the incorporation of more ion exchange groups, which increases ions' exchange capacity. This leads to an excessive water uptake and swelling of the membrane, caused by the strong coordination of water molecules around the ion exchange groups (quaternary ammonium).<sup>64</sup> Hydrophilic cross-linked membranes have shown a high water uptake and a relatively high swelling ratio (around 20%), but hydrophobic cross-linked membranes have shown a lower water uptake and swelling ratio (less than 5%). The low water uptake of the hydrophobic cross-linked membranes results in a reduction in ion exchange capacity and hydroxide conductivity.<sup>166</sup>

For the water uptake measurements, the membrane samples are first changed to the hydroxide form. After that, they are dried to a constant mass and weighed, and the length is measured. The membrane sample is then immersed at given temperatures for a duration of time (usually 24 hours) in a sealed bottle of water. The water uptake is measured in water previously degassed and blanketed with flowing Ar. After the immersion, the membranes are wiped quickly with laboratory tissue paper to remove excess surface water, and then immediately weighed and measured.<sup>88,94</sup> The obtained data are then used to calculate water uptake (WU) and swelling ratio (SR).<sup>98</sup>

**Chemical stability.** AEMs should be highly resistant toward oxidising and reducing species, as well as being stable during the development of membrane electrode assemblies (MEAs).<sup>65</sup> There have been many reports regarding the instability of AEMs in alkaline media, especially at elevated temperatures, so the chemical stability of AEMs needs to be improved.<sup>165</sup> Since a chemically stable AEM with sufficient durability is not commercially available, many polymer chemistries are under investigation in order to develop more stable AEMs.<sup>155</sup> Chemical stability of an AEM can be characterised by the determination of the swelling index and should be high, especially in alkaline pH.<sup>65</sup>

The majority of AEMs contain quaternary ammonium functional groups and have reasonable stability in alkaline media. It has been observed that benzyltrimethyl ammonium exchange sites are especially stable.<sup>157</sup> AEMs' instability in alkaline media can be attributed to the displacement of the ammonium group by OH<sup>-</sup> anions, as the latter are very good nucleophiles.<sup>157,165</sup> Sun *et al.*<sup>167</sup> compared various organic cations in terms of the alkaline stability and analogous cation-based AEMs. They included the chemical degradation mechanisms of quaternary ammonium cations, imidazolium, phosphonium, guanidinium, benzimidazolium and metal cations. The exchange reaction of hydroxide (OH<sup>-</sup>) with bicarbonate (HCO<sub>3</sub><sup>-</sup>) *via* attenuated total reflectance (ATR IR) spectroscopy can be used to determine chemical stability.<sup>160</sup> Oxidative stability can be determined with the exposure of a hydroxide form of a membrane to Fenton's reagent (1 ppm FeSO<sub>4</sub> in 3% H<sub>2</sub>O<sub>2</sub>), where the quality changes of the fully-dried AEM before and after the tests are recorded to evaluate the oxidative stability of the AEM.<sup>103</sup>

**Cell performance.** Cell performance depends on many parameters, such as type of fuel, the type and loading of the catalyst metal, the use of air or oxygen, operating temperature, relative humidity, addition of KOH to the fuel, fuel flow rate, presence of backpressure for the gas supply, MEA fabrication process, *etc.* Fuel cell characterisation techniques allow the quantitative comparison of different fuel cell systems, which enables the distinguishment between good and poor fuel cell designs. The performance of a fuel cell cannot be determined simply by summing the performances of its individual components, as there are losses due to the components themselves, as well as due to the interfaces between components. Therefore, in order to characterise a fuel cell, it is necessary to perform *in situ* testing, as *in situ* characterisation techniques provide a wealth of information about operational fuel cell behaviour.<sup>168</sup>

A fuel cell's overall performance is usually characterised by a polarisation curve (*j*-*V* curve) and power density. Power density (*P*) is given in mW cm<sup>-2</sup> and current density (*j*) is given in mA cm<sup>-2</sup>. The fuel cell *j*-*V* performance can change significantly, depending on factors like the operating conditions and testing procedures. Identical operating conditions, testing procedures and device histories need to be applied in order to obtain comparable performance results. The best way to gain understanding of why a fuel cell performs the way it does is to think of the fuel cell's performance in terms of the various major loss categories: activation loss, ohmic loss, concentration loss and leakage loss.<sup>168</sup> **Activation losses:** these losses are caused by the slowness of the reaction taking place on the surface of the electrodes. A proportion of the voltage generated is lost in driving the chemical reaction that transfers the electrons. **Ohmic losses:** the voltage-drop due to the resistance to the flow of electrons through the material of the electrodes. This loss varies linearly with current density. **Concentration losses:** losses that result from the change in concentration of the reactants at the surface of the electrodes as the fuel is used. **Fuel crossover losses:** losses that result from the waste of fuel passing through the electrolyte and electron conduction through the electrolyte. This loss is typically small, but can be important in low temperature cells.<sup>169</sup>



Based on experiments, temperature has an important effect on fuel cell performance, as it increases the reaction rate, diffusion phenomena and conductivity of the membrane.<sup>170</sup> In addition, the molarity and cathode and anode flow rate and cathode pressure have a significant effect on the performance of the fuel cell. Heyatiatab *et al.*<sup>170</sup> observed improved fuel cell performance with increased temperature and ethanol concentration. The flow rates of more than one stoichiometric coefficient had little effect on fuel cell performance, while increased cathode pressure caused oxygen concentration increase in the catalyst layer, and led to better oxygen reduction and reaction rate, and an increase in performance of a direct ethanol fuel cell.

For the measurement, a pilot fuel cell as a whole needs to be constructed with all the elements of a working fuel cell (*in situ* testing). Obtaining a polarisation curve ( $j$ - $V$  curve) is the most common method used to test a fuel cell's performance, and allows an easy comparison to other already published polarisation curves obtained under similar testing conditions. The  $j$ - $V$  curve displays the voltage output of the fuel cell for a given current density loading. They are usually obtained with a potentiostat or galvanostat, which draws a fixed current from the fuel cell and measures the fuel cell output voltage. The voltage response of the fuel cell can be determined by stepping up the load on the potentiostat slowly. In reality, fuel cells achieve their highest output voltage at open circuit (no load) conditions, and the voltage drops off with increasing current draw. This is known as polarisation. Another popular method is the electrochemical impedance spectroscopy, which is a more sophisticated method, but the drawback is that it is time consuming and the results are more difficult to interpret.<sup>171</sup>

**Performance stability.** The term performance stability means the stability of power density, which is linked strongly to the AEM and MEA, as well as to the fuel cell operating time, alkaline conditions and the fuel used. All of the components and operating conditions of the fuel cell need to be optimised to ensure a good and durable cell performance.<sup>172</sup> Performance stability studies are reported as operational tests of AEMFCs at constant current density or constant voltage, and show the corresponding performance stability data as cell voltage *versus* time. The durability of a fuel cell is a key performance factor, as the lifetime of the fuel cell needs to meet application expectations. The US Department of Energy set a durability with cycling target for 2020 to reach less than 10% drop in power after 5000 hours based on a polarisation curve and durability testing protocols at 80 °C for hydrogen fuel cells.<sup>173</sup> Therefore, their durability target for transportation fuel cells is 5000 hours and 40 000 hours for stationary application fuel cells under realistic operating conditions, which include: impurities in the fuel and air, starting and stopping, freezing and thawing, and humidity and load cycles that result in stresses on the chemical and mechanical stability of the fuel cell system materials and components.<sup>174</sup>

AEMFC degradation rates can increase substantially when the humidity level is low or at elevated cell temperatures (90 °C or higher). The main reason for the performance stability decay is the chemical degradation of the anion conducting ionomers used as AEMs and ionomers in the alkaline media present in the fuel cell. The stability of AEMs includes chemical and mechanical stabilities, which are affected by relative humidity

cycling, high operating temperature and chemical degradation of the backbone or functional groups. There are several mechanisms of chemical degradation of anion conducting moieties in alkaline media, which are described by Cermenek *et al.*<sup>65</sup> The chemical degradation causes a reduction in a membrane's conductivity, which increases the cell resistance and limits cell durability highly. This represents a major challenge that still needs to be overcome, so the research is now focused on the development of new polymer chemistries for the production of more stable AEMs.<sup>14</sup> The performance stability can be improved with a reduction in AEM thickness, and with the use of functional groups with increased stability properties. Dekel *et al.*<sup>175</sup> have shown a theoretical ability of achieving impressive cell lifetime by tuning these two parameters (AEM thickness and degradation kinetics of ionomeric materials) with a unique model capable of predicting the performance stability of AEMs.

Stability of the membranes in highly alkaline media (fuel cell operating conditions) is important; therefore, the alkaline stability of promising AEMs needs to be determined by immersion into an alkaline solution (usually 1 M NaOH or 1 M KOH), or in liquid fuel at a high temperature for a pre-determined time period. After that, the membrane samples are washed with deionised water several times, in order to remove residual OH<sup>-</sup> ions. The stability is then determined with a conductivity measurement or IEC, water uptake, swelling ratio determination for the membranes after exposure to alkali media in comparison to un-exposed membranes. Often these parameters are measured at certain alkaline treatment times, and a chart of alkaline stability over time is produced.<sup>101</sup>

However, the most important are durability tests, where the voltage drop of the MEA at fuel cell operating conditions is followed with time. In long-term durability tests the voltage is recorded over a continuous operating time with short intervals of off-periods. It is desired that a stable cell potential is obtained during the on cycles, and during the off periods the cell potential should immediately return to the open circuit voltage.<sup>132</sup> The durability of AEM fuel cells is still incomparable to PEM fuel cells, yet Qu *et al.*<sup>104</sup> recorded a constant discharge current for 52 h before dropping in a direct borohydride fuel cell. Zhang *et al.*<sup>95</sup> found no decline in cell performance over 80 h at 0.3 V at 60 °C for its polyolefin side-chain-type quaternary ammonium membrane, which shows excellent stability of MEA under fuel cell operating conditions. The effect of the fuel concentration was studied by Maya-Cornejo *et al.*<sup>176</sup> and has shown a decrease in the fuel cell performance with a higher concentration of fuel (1 M ethanol yielded higher power density than 3 M ethanol fuel). The decrease of performance at high ethanol concentrations is linked to a variation of ethanol oxidation selectivity in terms of reaction products' distribution, as a larger water content could result in an increase of CO<sub>2</sub> or CH<sub>3</sub>COOH yield. A similar effect was also observed in an ethylene glycol (EG) fuel cell,<sup>177</sup> where the power density increased when the fuel consisted of 1 M EG in comparison to 0.25 M EG, and decreased to the lowest value when 3 M EG was used. The observed effect is due to the feeding of 0.25 M EG not being able to achieve a sufficiently high mass transfer rate required at high current densities, which causes the EG





concentration in the anode catalyst layer to become insufficient. The 3 M EG feed is too concentrated, as it may cover the active sites in the anode catalyst layer, which prevents the OH<sup>-</sup> adsorption, which slows down the reaction. Also, the effect of alkali added to fuel studied as KOH present in ethanol fuel feed, was studied by Maya-Cornejo *et al.*<sup>176</sup> They observed an increase in power density by 1 M KOH in comparison to 0.3 M KOH, but with increasing the concentration to 3 M KOH the power density decreased, and was even lower than with 0.3 M KOH.

### 3. Fuels used in alkaline membrane fuel cells

A wide range of liquid and solid fuels may be used in a heat-engine system, while hydrogen, methanol and ethanol are the primary fuels available for current fuel cells.

#### 3.1. Hydrogen fuel

Hydrogen is the most abundant element, and accounts for approximately 15 mol% on the surface of the earth (water, fossil fuels, biomass). Molecular hydrogen is a gas at ambient conditions, and is very difficult to condense as it has a very low critical point. It has the potential for very high energy densities relevant for mobile applications.<sup>178</sup> Most hydrogen is currently produced by steam reforming of hydrocarbons. It can also be produced by heating coal to about 1000 °C in the absence of oxygen, by partial burning of coal in the presence of steam, or by electrolysis. With the production from coal a mixture of hydrogen with CO, CO<sub>2</sub> and other gasses are obtained, which need to be separated to obtain pure hydrogen. The generation of CO<sub>2</sub> can be avoided if the electricity is generated from nuclear, hydroelectric, wind, solar or geothermal energy. It is a very desired fuel, as the only product of hydrogen oxidation is water.<sup>179</sup> The future price of the hydrogen fuel is uncertain, but the National Renewable Energy Laboratory (USA) estimates that hydrogen fuel prices may fall to the 10 USD to 8 USD per kg price range in the 2020 to 2050 period.<sup>180</sup> The advantages and disadvantages of hydrogen *versus* ethanol used as a fuel for fuel cells are discussed in the ethanol fuel section.

Reactions in an alkaline anion exchange fuel cell operating on hydrogen fuel:

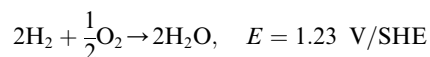
Anode:



Cathode:



Overall:<sup>165</sup>



Zhang Z. *et al.*<sup>88</sup> prepared AEMs based on one-step benzyla-tion modification of commercial poly(ether ether ketone). The performance of such a membrane has been tested in an H<sub>2</sub>/O<sub>2</sub> single cell operated at 70 °C, where the peak power density of 391 mW cm<sup>-2</sup> has been observed (100% relative humidity, without backpressure for both feed gases and Pt/C catalysts on both electrodes). Li *et al.*<sup>90</sup> prepared an imidazolium functionalised PEEKK AEM, which achieved a maximum power density of 46.16 mW cm<sup>-2</sup> at 60 °C in an H<sub>2</sub>/O<sub>2</sub> single cell. The humidity was 100% and back pressure 0.1 MPa for both feeds. A tetraalkylammonium-functionalised fluoropolyolefin AEM prepared by Zhang X.<sup>95</sup> yielded a power density of 133 mW cm<sup>-2</sup> at 60 °C with Pt/C catalysts in an H<sub>2</sub>/O<sub>2</sub> single cell without back pressure. A series of polystyrene-grafted PPO with pendant quaternary ammonium groups were synthesised as AEMs by Yang *et al.*<sup>98</sup> Performance tests in an H<sub>2</sub>/O<sub>2</sub> single cell (100% relative humidity, Pt/C catalysts) have shown a power density of 64.4 mW cm<sup>-2</sup> at 60 °C. Modified PPO AEMs were also prepared by Zhu *et al.*<sup>101</sup> with the aim to study the effect of inclusion of rotatable ethylene spacers on the PPO based membrane's performance in an AEMFC. H<sub>2</sub>/O<sub>2</sub> single cell tests have shown a maximum power density of 437 mW cm<sup>-2</sup> at 65 °C (PtRu/C anode and Pt/C cathode with 100% humidity of gaseous feeds). Another PPO based AEM was prepared by Lin *et al.*<sup>102</sup> The AEM had PPO chains linked to pendant 1,2-dimethylimidazolium, and produced a maximum power density of 56 mW cm<sup>-2</sup> in an H<sub>2</sub>/O<sub>2</sub> single cell at 35 °C with Pt/C catalysts. Another research group, Lim *et al.*,<sup>99</sup> focused on PPO based AEMs with the intention to identify the most suitable headgroup. A series of PPO based AEMs with four of the most widely investigated head groups were prepared, those being quaternary ammonium, imidazolium, piperidinium and morpholinium. The prepared AEMs were tested in an H<sub>2</sub>/O<sub>2</sub> single cell at 60 °C and 95% relative humidity with Pt/C as catalysts. The highest power density was noted for the quaternary ammonium headgroup PPO at 155 mW cm<sup>-2</sup>, followed by the morpholinium headgroup PPO at 110 mW cm<sup>-2</sup>, the piperidinium headgroup PPO at 100 mW cm<sup>-2</sup> and the lowest at 40 mW cm<sup>-2</sup> for the imidazolium headgroup PPO. Yu *et al.*<sup>106</sup> prepared double cross-linked AEMs based on PBI and poly(vinylbenzyl chloride) (PVBC) with *N,N,N',N'*-tetramethyl-1,6-hexanediamine as a quaternising agent with different ratios of PBI and PVBC. The AEM produced from an equal mass ratio of PBI and PVBC reached a power density of 244.93 mW cm<sup>-2</sup> at 60 °C in an H<sub>2</sub>/O<sub>2</sub> single cell. Pt/C was used as the cathode catalyst and PtRu/C as the anode catalyst, and the feeds were supplied at 100% relative humidity with 0.2 MPa back pressure. Ponce-González *et al.*<sup>93</sup> investigated the performance of a benzyl quaternary ammonium functional group in AEMs. They prepared AEMs containing saturated-heterocyclic benzyl-quaternary ammonium groups synthesised by radiation grafting onto ETFE films. An H<sub>2</sub>/O<sub>2</sub> single cell containing such a membrane yielded a power density of 630 mW cm<sup>-2</sup> at 60 °C with PtRu/C anodes, Pt/C cathodes and polysulfone ionomer (feeds with 100% relative humidity and no backpressure). The performances of some natural based AEMs have also been studied, including a composite membrane from 2 wt% quaternised CNC and



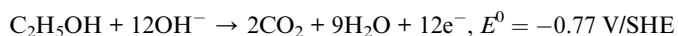
quaternised PPO, which was prepared by Cheng *et al.*<sup>139</sup> The H<sub>2</sub>/O<sub>2</sub> cell performance of such a membrane showed an impressive peak power density of 392 mW cm<sup>-2</sup> at 60 °C with no back-pressure on the feed gases and a Pt/C cathode and PtRu/C anode. Zhou *et al.*<sup>121</sup> fabricated a novel OH<sup>-</sup> conducting membrane composed of CS, an ionised organic compound and hydroxylated multiwalled carbon nanotubes cross-linked by glutaraldehyde. H<sub>2</sub>/O<sub>2</sub> single cell tests have shown a power density of 31.6 mW cm<sup>-2</sup> at room temperature with Pt/C catalysts. Another AEM based on CS was investigated by Zhou *et al.*<sup>119</sup> They produced a CS modified by polymeric reactive dyes containing quaternary ammonium groups AEM, which produced a power density of 29.1 mW cm<sup>-2</sup> at 25 °C in a H<sub>2</sub>/O<sub>2</sub> cell with Pt/C catalysts.

### 3.2. Ethanol fuel

Ethanol is the second simplest alcohol, right after methanol, as it contains two carbon atoms and has an energy density of 8030 W h kg<sup>-1</sup>.<sup>164</sup> It contains one OH group and one C–C bond. Because of the C–C bond, the complete oxidation of ethanol is difficult, and the oxidation reaction occurs at a lower rate. This problem can be solved by increasing the fuel cell's operating temperature (around 90 °C), although if the temperature is too high, the membrane can suffer from dehydration. The otherwise slow ethanol electro-oxidation causes cell voltage drops at low current densities.<sup>18</sup> Complete electro-oxidation of ethanol has not yet been achieved, but several catalysts are being investigated. It has been reported that CuNi-modified Pt/Ru catalysts have shown superior ethanol oxidation in alkaline media in comparison to acidic media. Catalysts capable of complete oxidation of ethanol in alkaline media still need to be found in order to maximise the energy extraction from ethanol fuel. Good performance at lower temperatures needs to be obtained in order for the fuel to be applicable in portable electronic devices.<sup>165</sup>

Reactions in an alkaline anion exchange fuel cell: (the total oxidation of ethanol).

Anode:



Cathode:



Overall:<sup>181,182</sup>



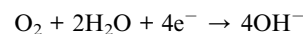
In the incomplete ethanol oxidation reaction, the predominant product is acetic acid and not carbon dioxide. Therefore, the electron transfer number is reduced to 4 electrons per one ethanol molecule instead of 12 electrons per one ethanol

molecule for complete ethanol oxidation, making the electron transfer rate lower.

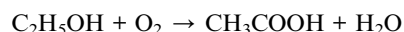
Anode:



Cathode:



Overall:<sup>65</sup>



Ethanol is renewable, more than methanol, as it can be produced from sugar containing raw materials from biomass or agricultural products. As for these benefits, and the benefits stated in the subchapter below, ethanol is considered as a very promising fuel for direct alkaline anion exchange membrane fuel cells, and many research groups have focused on fuel cells running on ethanol.<sup>164</sup>

Zakaria and Kamarudin<sup>183</sup> studied the performance of an electrolyte membrane based on quaternised PVA polymer in passive alkaline direct ethanol fuel cells (DEFC). The composition of the quaternised PVA-based membranes was optimised with potassium hydroxide (KOH) as an ion charge carrier and by incorporating filler graphene oxide (GO). The DEFC operated on 2 M ethanol with 2 M KOH at different temperatures with a membrane in a hydrated state, and Pt was used as the cathode catalyst and PtRu as the anode catalyst. They noted an increase in power densities with increasing temperature, 11.3 mW cm<sup>-2</sup> at 30 °C, 13.5 mW cm<sup>-2</sup> at 60 °C and 19.3 mW cm<sup>-2</sup> at 90 °C. Zakaria *et al.*<sup>184</sup> also investigated the performance of a cross-linked quaternised PVA/GO composite membrane in a DEFC. The DEFC operating conditions were the same as in the previous article, and the DEFC received air as the cathode feed. At 30 °C a maximum power density of 9.1 mW cm<sup>-2</sup> was noted, and at 60 °C a higher power density has been noted of 11.4 mW cm<sup>-2</sup>. For Fuku *et al.*<sup>185</sup> the main objective was to synthesise and study a bio-inspired metal oxide-support catalyst which would enhance CO<sub>2</sub> reduction, fuel cell performance and ethanol oxidation. The fuel cell operated on 1 M ethanol with 1 M KOH at 25 °C with a N15 A201 Tokuyama commercial membrane and air as the cathode feed. A power density of 18 mW cm<sup>-2</sup> has been achieved with an FeCo/C cathode and a commercial Pd/C anode, but an increased power density of 26 mW cm<sup>-2</sup> has been achieved with an anode nanocatalyst Pd–NiO/C and Pd/C cathode. Herranz *et al.*<sup>186</sup> tested a series of PVA : PBI membranes with different ratios of PVA and PBI. The highest power density was noted with a PVA and PBI 4 : 1 ratio, and it was 76 mW cm<sup>-2</sup> at 90 °C with a Pt cathode and a PtRu anode. The fuel consisted of 2 M ethanol and 2 M KOH, and oxygen with a back pressure of 0.5 atm was used as the cathode feed. Maya-Cornejo *et al.*<sup>176</sup> conducted power density measurements in a fuel cell at 60 °C with different anode catalysts. A power density of



7.1 mW cm<sup>-2</sup> was achieved with a Pt/C anode and Pt black cathode, but a power density of 14.2 mW cm<sup>-2</sup> was measured when the anode catalyst was switched to PtCu/C. In both experiments, the fuel cell contained an A201 Tokuyama AEM, and operated on 1 M ethanol as fuel and pure oxygen with 100% humidity as the cathode feed. With the addition of 1 M KOH to the fuel the fuel cell exhibited a power density of 15.2 mW cm<sup>-2</sup>. Ma *et al.*<sup>187</sup> used a bimetallic Pd<sub>3</sub>Ru/C anode catalyst to showcase a peak power density as high as 176 mW cm<sup>-2</sup> in an AEM DEFC at 80 °C, which was about 1.8 times higher than that using the single metal Pd/C catalyst. The DEFC had an A201 Tokuyama AEM with a fuel feed comprising of 3 M ethanol and 3 M KOH, with dried oxygen gas as cathode feed. Dutta and Datta<sup>188</sup> reported a power density of 51 mW cm<sup>-2</sup> in a DEFC with a Pt/C cathode and Pd<sub>41</sub>Ni<sub>29</sub>Au<sub>30</sub>/C anode at 40 °C. The fuel cell contained an A006 Tokuyama membrane, and ran on 1 M ethanol with 0.5 M NaOH as fuel and a pure oxygen cathode feed. Li *et al.*<sup>189</sup> designed and investigated an air-breathing direct ethanol fuel cell with an A201 Tokuyama AEM. The cell yielded a power density of 38 mW cm<sup>-2</sup> with an Fe–Cu–N<sub>4</sub>/C cathode and PdNi anode at room temperature. Fujiwara *et al.*<sup>190</sup> concluded that the power density increased significantly in a DEFC from 6 mW cm<sup>-2</sup> to 58 mW cm<sup>-2</sup> at room temperature and atmospheric pressure when the electrolyte membrane was changed from CEM to AEM (Pt black cathode and PtRu black anode). The fuel feed consisted of 1 M ethanol and 0.5 M KOH and humidified gas as the cathode feed, and the cell had an AEM from Tokuyama. A composite consisting of quaternised PVA and 5% quaternised CS nano particle was prepared by Liao *et al.*<sup>132</sup> It was tested in an ethanol fuel cell and achieved a power density of 59.17 mW cm<sup>-2</sup> at 60 °C when fed with 3 M ethanol with 5 M KOH, and contained Pt/C as the cathode catalyst and PtRu/C as the anode catalyst. Kaker *et al.*<sup>70</sup> utilised a CS–Mg(OH)<sub>2</sub> based nanocomposite membrane in a direct ethanol fuel cell with an PtRu/C anode and Pt/C cathode. Such a cell achieved a power density of 72.7 mW cm<sup>-2</sup> at 80 °C when fed with 3 M ethanol in 5 M KOH.

Current commercially available fuel cells run on hydrogen in acidic media. Hydrogen can be stored directly or produced in the appliance by reforming sources of hydrogen (methanol, hydrocarbon fuels derived from crude oil *e.g.*, gasoline, diesel, or middle distillates).<sup>191</sup> The main drawbacks with commercialisation of hydrogen fuel cells are the transport and currently insufficient storage infrastructure of the gaseous hydrogen fuel. The storage of hydrogen is quite a complicated technological procedure. The mere technical execution is complicated, and the safety measures need to be applied for storing explosive gases. Another drawback is the economically unviable production of hydrogen at the moment.<sup>192</sup> The substitution of hydrogen with biofuels such as methanol and ethanol, eliminates difficulties with the transportation and storage of the fuel. The use of biofuels in fuel cells enables the production of electricity with little or no CO<sub>2</sub> emissions, which helps to keep low CO<sub>2</sub> levels in the atmosphere.<sup>181</sup> Alkaline media are more suitable for the oxidation of ethanol in comparison to acidic media. The oxidation rate is lower in acidic media and carbon by products are formed, which absorb to the active sites on the catalyst. When the active sites of the catalyst are occupied the efficiency of the fuel cell decreases.

In accordance with the presented benefits, there has been increased research activity on the development of alkaline fuel cells operating on methanol and ethanol. Methanol is the simplest alcohol, and does not contain any carbon–carbon bonds, which makes it easier to oxidise than other alcohols. The drawback of methanol is that it is toxic and, therefore, unsafe for consumer use. The kinetics of the anode reaction when methanol is used in alkaline fuel cells are slow, and DMFC also suffer from abundant methanol crossover and low performance.<sup>192</sup> Ethanol is a promising fuel for alkaline fuel cells, as it has a low toxicity, a higher energy density (6.3 kW h L<sup>-1</sup>) than methanol (4.8 kW h L<sup>-1</sup>) and can be produced readily from biomass with fermentation in great quantities with little impact on the environment.<sup>192,193</sup> Ethanol also has a higher boiling point and lower vapour pressure than methanol.<sup>194</sup>

The production of ethanol is possible from sucrose-containing feedstock, lignocellulosic biomass and starchy materials.<sup>195</sup> Currently, bioethanol is produced mainly from sugar, starch, cellulose and hemicellulose, as well as from holocellulose found in the cell walls of algal biomass. While lignocellulose is an abundant and cheap source, the conversion of biomass to ethanol has higher costs than other feedstock.<sup>196</sup> Ethanol production from food sources is also not viable, as that would increase the food price and lessen the amount of land available for food production. From this perspective, algal biomass is a promising source for ethanol production.

Ethanol can be produced from sugar cane, corn, beets, wheat, soy, algae,<sup>196</sup> as well as from organic materials which contain cellulose, such as wood biomass, pellets and agro-industry waste, organic waste *etc.*<sup>181</sup> The production of ethanol from renewable sources is carried out *via* anaerobic digestion, and is a simpler process than the production of methanol, which is obtained by the foregoing biomass gasification.<sup>194</sup> Table 3 sums up the advantages and disadvantages of ethanol and hydrogen as a fuel for fuel cells.

### 3.3. Methanol

Methanol is the simplest alcohol, with only one carbon atom and only one OH group, therefore, it is easier to oxidise than ethanol. It has good electrochemical activity and is consistently available, biodegradable, relatively cheap, and it can be handled, transported and stored easily. Methanol is far more toxic than ethanol, but still methanol's toxicity is considered to be low, within an acceptable range. Special precautions for handling methanol need to be undertaken. It has a high energy to carbon ratio and an energy density of 4820 W h L<sup>-1</sup>.<sup>164</sup>

Reactions in an alkaline anion exchange fuel cell:

Anode:



Cathode:



Overall:<sup>182</sup>



In DMFC, an incomplete oxidation reaction results in the production of carbon monoxide in trace amounts, which is poisonous to the Pt anode electro-catalyst. The carbon monoxide needs to be removed from the anode constantly in order to prevent catalyst poisoning.<sup>164</sup>

Jurzinsky *et al.*<sup>197</sup> studied the performance of an A201 Tokuyama in a AEMFC operating on 1 M methanol with 2 M KOH. They observed a power density of 4.8 mW cm<sup>-2</sup> at 60 °C with Pd/C as the anode and cathode catalysts, and synthetic air as the cathode feed. A fuel cell utilising the same membrane and temperature achieved a power density of 16.5 mW cm<sup>-2</sup> with bimetallic PdRh/C catalysts. With an increase of temperature to 80 °C and an increase in alcohol concentration in the fuel to 4 M methanol with 2 M KOH, the power density increased to 104.9 mW cm<sup>-2</sup> for PdRh/C bimetallic catalysts. The same membrane in a methanol fuel cell was also studied by the same group<sup>198</sup> with a different bimetallic catalyst, Pd<sub>3</sub>Ag/C, which achieved a lower power density of 11.9 mW cm<sup>-2</sup> at 60 °C when 2 M methanol with 2 M KOH was used as the anode feed. Jurzinsky *et al.*<sup>199</sup> also obtained a power density of 14.3 mW cm<sup>-2</sup> at 60 °C with the same membrane in a fuel cell operating on 4 M methanol Pt/C with a comb-like ionomer anode catalyst and Pt/C on the cathode with oxygen feed. Kim *et al.*<sup>50</sup> tested a Tokuyama AEM and obtained a power density of 6.8 mW cm<sup>-2</sup> at ambient temperature with a Pt/C cathode and PtRu/C anode catalyst with 1 M methanol and 1 M KOH fuel. In comparison, a Nafion 117 membrane produced a power density of 5.2 mW cm<sup>-2</sup> with the same catalysts and methanol as fuel. A PVA AEM achieved a power density of 18.5 mW cm<sup>-2</sup> at 60 °C.<sup>200</sup> The fuel cell operated on 2 M methanol with 5 M KOH at a flow of 5 mL min<sup>-1</sup> and humidified oxygen as the cathode feed at 100 mL min<sup>-1</sup>, both utilising Pt/C catalysts. An improvement was noted when PVA was blended with graphene, as the blended membrane produced an increased power density of 45.8 mW cm<sup>-2</sup> under the same testing conditions. He *et al.*<sup>201</sup> produced a novel quaternary ammonium functional AEM which exhibited

a power density of only 14 mW cm<sup>-2</sup> at 80 °C on Pt/C catalysts and methanol as fuel and air as the cathode feed. The membrane was a quaternary ammonium functional addition-type with norbornene copolymer, which had different alkyl side chain length comb-shaped structures or different contents of 2-(4-phenyl-butoxymethyl)-5-norbornene. A composite consisting of quaternised PVA and 5% quaternised CS nano particle was prepared by Liao *et al.*<sup>132</sup> It was also tested (previously in an ethanol fuel cell) in a methanol fuel cell, and achieved a power density of 73 mW cm<sup>-2</sup> at 60 °C when fed with 2 M methanol in 6 M KOH solution, and contained Pt/C as the cathode catalyst and PtRu/C as the anode catalyst. Li *et al.*<sup>134</sup> designed a CS nanoparticle-incorporated quaternised PVA composite membrane for direct methanol alkaline fuel cells. The peak power density reached 67 mW cm<sup>-2</sup> at 80 °C when fed with 1 M methanol in 6 M KOH at the anode and oxygen as the cathode feed. PVA/CS membranes were also studied by Yang *et al.*,<sup>136</sup> being PVA/CS solution casting and PVA/CS electrospun nanofibre membranes, cross-linked by glutaraldehyde. Both membranes were tested in a methanol fuel cell with 2 M methanol and 2 M KOH as the anode feed and oxygen as the cathode feed, and E-TEK Pt–Ru black catalysts. The solution casting membrane reached a power density of 19.4 mW cm<sup>-2</sup> and the electrospun 30 mW cm<sup>-2</sup> at 50 °C. A composite quaternary phosphonium polymer microsphere, cross-linked and with dense carriers incorporated into CS AEM, was prepared by Liu and Sun.<sup>124</sup> The methanol fuel cell test provided a power density of 110 mW cm<sup>-2</sup> at 60 °C. The cathode was fed with oxygen at 100% relative humidity, and the anode was supplied with 3 M KOH and 1 M methanol solution. PtRu/C was employed as the anode catalyst and Pt/C as the cathode catalyst.

### 3.4. Hydrazine

Hydrazine as fuel for alkaline fuel cells has been studied since the 1970s.<sup>202</sup> Hydrazine (N<sub>2</sub>H<sub>4</sub>) is a colourless liquid. The oxidation reaction of hydrazine does not result in any CO<sub>2</sub> production, therefore, the possibility of poisoning the anode is eliminated (carbon atoms can poison the anode catalyst), which leads to a longer life of the catalyst. The use of a Pt catalyst is still the most suitable, as hydrazine oxidises and decomposes at the anode, and Pt provides the lowest decomposition rate.

**Table 3** Advantages and disadvantages of ethanol and hydrogen used as fuel in fuel cells

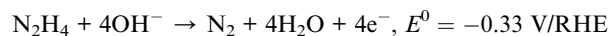
|               | Ethanol   | Hydrogen   |
|---------------|---|--|
| Advantages    | <ul style="list-style-type: none"> <li>– Green, low emission fuel when produced as bio ethanol</li> <li>– The toxicity is very low</li> <li>– A higher energy density as methanol</li> <li>– Renewable, can be produced readily from biomass</li> </ul> | <ul style="list-style-type: none"> <li>– Green, no CO<sub>2</sub> emissions from the fuel cell, water is the only product</li> </ul>   |
| Disadvantages | <ul style="list-style-type: none"> <li>– CO<sub>2</sub> emissions from the fuel cell</li> <li>– Expensive in comparison to gasoline</li> <li>– If produced from crops it requires a lot of land which could be used for food production</li> </ul>      | <ul style="list-style-type: none"> <li>– Difficult to produce</li> <li>– Currently a lot of hydrogen is produced from fossil fuels</li> <li>– A highly explosive gas</li> <li>– Storage and transportation are technologically complicated</li> <li>– Currently it is economically unviable</li> </ul> |



Although the use of non-noble catalysts is possible, Pt is still the preferred one. The theoretical mass energy density of hydrazine is  $2.6 \text{ kW h kg}^{-1}$ . It is alkaline in aqueous solution, and expected to be very compatible with an AEM.<sup>165</sup> Out of all the known fuels possible to fuel direct liquid fuel cells, hydrazine is considered as the most toxic to humans, as it can damage the lungs, kidneys and the central nervous system, and is also expensive.<sup>164</sup> To tackle these issues, the Daihatsu Motor company has developed a method for safe storage of hydrazine in the form of solid hydrazone ( $\text{>C=N-NH}_2$ ), which does not exhibit mutagenic properties, and its solid nature is much safer in the event of tank damage. The hydrazine can be released from the hydrazone form by adding a solvent into the fuel tank.<sup>202</sup>

Reactions in an alkaline anion exchange fuel cell:

Anode:



Cathode:



Overall:<sup>43,203</sup>



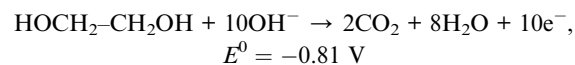
A power density of  $230 \text{ mW cm}^{-2}$  has been noted by Yoshimura *et al.*<sup>94</sup> with a polyvinylimidazolium hydroxide-grafted AEM with a fuel cell operating on 10% hydrazine hydrate in 1 M KOH at  $80^\circ\text{C}$  with air (the cathode catalyst: Co-PPY/C and anode:  $\text{Ni}_{0.9}\text{La}_{0.2}$ ). In a different work, Yoshimura *et al.*<sup>204</sup> noted a power density of  $75 \text{ mW cm}^{-2}$  for a copoly(1-vinyl-3-propylimidazolium hydroxide/styrene/ethylene)-grafted (ETFE) AEM with a fuel cell operating on 5% hydrazine hydrate in 1 M KOH at  $80^\circ\text{C}$  with humidified air (the cathode catalyst: Co-PPY/C and anode:  $\text{Ni}_{0.9}\text{La}_{0.1}$ ). Qin *et al.*<sup>205</sup> noted a power density of  $64 \text{ mW cm}^{-2}$  with a fuel cell operating on 10% hydrazine hydrate, 5%  $\text{NaBH}_4$  and 10% NaOH at  $80^\circ\text{C}$  with Pt on carbon as the cathode catalyst and a composite anode catalyst.

### 3.5. Ethylene glycol

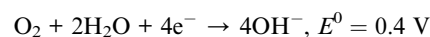
Ethylene glycol is an alcohol with two carbons and two OH groups. It has better properties than a single OH group alcohol, as it has a higher vapour pressure, which minimises fuel loss due to evaporation.<sup>164</sup> High electro-activity has already been observed of ethylene glycol in alkaline media. It has superior performance and power densities in AAEMFCs in comparison to methanol, but it has not yet been investigated to which degree ethylene glycol oxidises.<sup>165</sup> Ethylene glycol is used widely as antifreeze and for polyethylene terephthalate, so it has an already well established supply chain.<sup>164,165</sup> The ethylene glycol electro-oxidation reaction can form glycol-aldehyde, glycolate, glyoxylate, oxalate and CO/carbonates in alkaline media, depending on the catalysts used.<sup>206</sup> The theoretical oxidation

reaction on the anode and on the cathode is written below. In the case that the main product of oxidation reaction is oxalate, the electron transfer rate reaches 80% of the theoretical where the main product is  $\text{CO}_2$ .

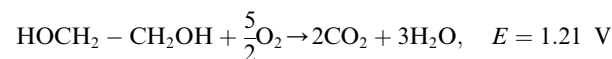
Anode:



Cathode:<sup>182</sup>



Overall:<sup>207</sup>

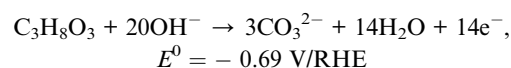


Jurzinsky *et al.*<sup>198</sup> tested an A201 Tokuyama AEM with different anode catalysts and a commercial Acta 4020 cathode catalyst in a fuel cell operating on 1 M ethylene glycol and 2 M KOH at  $60^\circ\text{C}$  with synthetic air. With Pd/C as the anode catalyst a power density of  $24.2 \text{ mW cm}^{-2}$  was noted, and a power density of  $39.3 \text{ mW cm}^{-2}$  was noted with  $\text{Pd}_3\text{Ag/C}$  as the anode catalyst. A power density of  $71 \text{ mW cm}^{-2}$  has been noted by Xin *et al.*<sup>208</sup> with an A201 Tokuyama AEM in a fuel cell operating on 0.1 M ethylene glycol with 2 M KOH at  $50^\circ\text{C}$  with oxygen and 30 psi back pressure (the cathode catalyst: Fe-Cu- $\text{N}_4/\text{C}$  and anode: Pt/C). An and Chen have provided an extensive review<sup>207</sup> of alkaline direct ethylene glycol fuel cell performances reported in the literature. They pointed out a maximum power density of  $112 \text{ mW cm}^{-2}$  at  $90^\circ\text{C}$  achieved by ref. 209. The fuel cell utilised an alkali doped polybenzimidazole AEM and Pd-Ni/C anode catalysts and non-Pt HYPERMEC cathode catalyst, and operated on 1 M ethylene glycol and 7 M KOH solution as the anode feed and dry pure oxygen as the cathode feed.

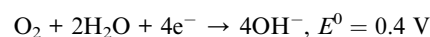
### 3.6. Glycerol

Glycerol is a non-toxic, non-volatile, non-flammable, cheap and bio-renewable alcohol. Not a lot of research has been conducted on the topic direct glycerol fuel cells, as it is still in an early research phase. Glycerol is produced as a by-product in the production of biodiesel, and it is produced in greater quantities than the current demand, so the price is low. The price of crude glycerol is cheaper than methanol and ethanol, and the theoretical energy density is  $6.4 \text{ kW h L}^{-1}$ .<sup>164</sup>

Anode:<sup>38</sup>



Cathode:<sup>182</sup>

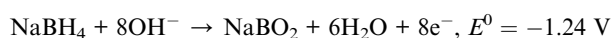


Zhang *et al.*<sup>210</sup> tested an A201 Tokuyama AEM with high purity glycerol and crude glycerol in an alkaline anion exchange membrane. With 1 M high purity glycerol they achieved a power density of 57.9 mW cm<sup>-2</sup> with Fe-Cu-N<sub>4</sub>/C as the cathode catalyst and Au/C as the anode catalyst at 80 °C, and oxygen with 30 psi back pressure. With 1 M crude glycerol and 2 M KOH at the same conditions as with high purity glycerol, they achieved a power density of 30.7 mW cm<sup>-2</sup>. Benipal *et al.*<sup>211</sup> studied the performance of a direct glycerol fuel cell with PTFE thin film separator. They achieved a power density of 214.7 mW cm<sup>-2</sup> with 1 M glycerol and 6 M KOH as fuel, and an Fe-based cathode catalyst and PdAg/carbon nanotubes as the anode catalyst at 80 °C. Wang *et al.*<sup>212</sup> tested an A201 Tokuyama AEM with different cathode catalysts in an alkaline anion exchange membrane with high purity glycerol at 80 °C operational temperature. Pt/C was used as the anode catalyst, and a power density of 86 mW cm<sup>-2</sup> was achieved with Ag nanoparticles on carbon black as the cathode catalyst. A power density of 45 mW cm<sup>-2</sup> was achieved when the same anode catalyst was used, but the cathode catalyst was replaced with Ag/C.

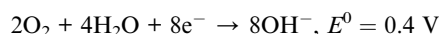
### 3.7. Borohydride

Borohydride contains no carbon items, so, like hydrazine, it produces no carbon products which could poison the anode catalyst. It is possible to use non-noble metal catalysts for the oxidation reaction, as sodium borohydride produces a high open circuit potential and achieves high power densities.<sup>165</sup> The drawback of borohydride is its toxicity, which poses a problem for commercialisation. Direct borohydride fuel cells can operate under an alkaline environment only, due to the instability of BH<sub>4</sub><sup>-</sup> in acidic and neutral conditions.<sup>164</sup> Borohydride has a theoretical maximum energy density of 9.3 kW h kg<sup>-1</sup>.<sup>165</sup>

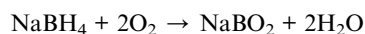
Anode:



Cathode:<sup>182</sup>



Overall:<sup>213</sup>



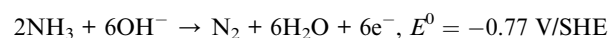
Qu *et al.*<sup>104</sup> fabricated a bi-guanidinium bridged polysilsequioxane composite AEM and tested it in a direct borohydride fuel cell. It yielded a peak power density of 321 mW cm<sup>-2</sup> at 40 °C with oxygen as the cathode feed and a fuel feed comprised of 1 M NaBH<sub>4</sub> and 3 M NaOH (Pt/C was utilised as the cathode and anode catalyst). Qin *et al.*<sup>214</sup> introduced a novel hydroxide anion exchange membrane composed mainly of poly(vinyl alcohol) and alkaline exchange resin (PVA-AER), and the same membrane impregnated with Co (Co-impregnated

PVA-AER). The testing conditions were the same for both types of membrane, being, 5 wt% NaBH<sub>4</sub> and 10 wt% NaOH at 60 °C as fuel, and humidified oxygen with a back-pressure of 0.2 MPa as the cathode feed. Co(OH)<sub>2</sub>-PPy-BP was used as the cathode and anode catalyst in both cases. A power density of 283 mW cm<sup>-2</sup> was obtained with the PVA-AER membrane, and a power density of 117 mW cm<sup>-2</sup> was obtained with the Co-impregnated PVA-AER membrane.

### 3.8. Ammonia

It is possible to utilise ammonia as a direct fuel for ammonium fuel cells, as well as an indirect fuel for hydrogen fuel cells. Ammonia is environmentally benign (used as fertiliser, to neutralise acid rain), and it is cheap, at 1.2 USD kW h<sup>-1</sup>.<sup>165</sup> It has advantageous properties over hydrogen, such as a higher boiling point and higher density, and is easier to store and transport.<sup>215</sup> Liquid ammonia is an excellent low-temperature fuel, as it has 70% more hydrogen content and 50% higher specific energy density than liquid hydrogen per unit of volume.<sup>216</sup>

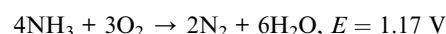
Anode:



Cathode:



Overall:<sup>182,217</sup>



Suzuki *et al.*<sup>218</sup> investigated an ammonia fuel cell employing an A201 Tokuyama AEM. The cell tests were conducted with a Pt/C cathode catalyst and different anode catalysts, being Pt/C, PtRu/C and Ru/C. The current densities achieved by these fuel cells were about one order of magnitude smaller than for the same fuel cells fed with hydrogen fuel. The cell with Pt/C exhibited higher current density than the cell with Pt-Ru/C, and Ru/C the lowest. The current densities for ammonia fuel cells were measured at 50 °C, and ammonia as an anode feed and oxygen/nitrogen mixture feed on the cathode. Siddiqui and Dincer<sup>219</sup> investigated an alkaline fuel cell operating on ammonia with a solid AEM. The AEM had a gel polystyrene cross-linked with divinylbenzene structure with quaternary ammonium as the functional group. The fuel cell employed Pt black catalysts, and, at the anode, was fed with pressurised (1 bar) ammonia gas, and the cathode with humidified air. The peak power density of such a fuel cell was found to be 6.4 W m<sup>-2</sup> at 25 °C. Silva *et al.*<sup>216</sup> achieved a maximum power density of 2.64 mW cm<sup>-2</sup> at 40 °C in a DAFC fed with ammonium hydroxide. The single cell was fed with 5 M NH<sub>4</sub>OH in 1 M KOH at the anode and oxygen at the cathode, and utilised a PtAu/C anode and Pt/C cathode catalyst and a Nafion 117 AEM. The same group<sup>220</sup> also ran single cell tests under identical conditions as previously, but

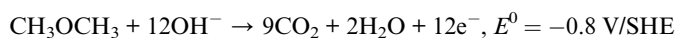


with a different anode catalyst (PtIr/C 50 : 50). Such a cell produced a power density of  $4.17 \text{ mW cm}^{-2}$  at  $40 \text{ }^\circ\text{C}$ .

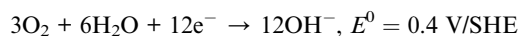
### 3.9. Dimethyl ether

Dimethyl ether is believed to be a promising fuel without NO<sub>x</sub> and SO<sub>x</sub> emissions, as well as no issues with production infrastructure and transportation.<sup>221</sup> Dimethyl ether is the simplest ether, and it is volatile but non-carcinogenic, non-toxic, non-teratogenic, non-mutagenic, and also less toxic than methanol. In nature it exists as a gas, and it can be utilised in a fuel cell in a gaseous or liquid form. The level of toxicity is low, but the side products of oxidation can be formaldehyde and methanol, which can be oxidised further.<sup>164</sup> 1 mol of dimethyl ether theoretically produces 12 mol electrons, twice that of methanol with 6 mol electrons, and so shows higher energy density than methanol. It also possesses low fuel crossover due to the low dipole moment, which is favourable to fuel cell applications.<sup>221</sup>

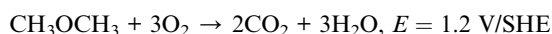
Anode:



Cathode:



Overall:<sup>182</sup>

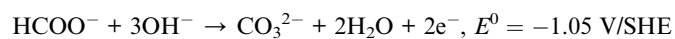


Xu *et al.*<sup>222</sup> assembled direct dimethyl ether fuel cells with a Nafion 117 AEM. Dimethyl ether with the addition of 1 M NaOH was used as the fuel, and humidified oxygen at ambient pressure was used as the cathode feed. A power density of  $60 \text{ mW cm}^{-2}$  was noted at  $80 \text{ }^\circ\text{C}$  with a Pt/C cathode catalyst and Pt-Ru/C anode catalyst.

### 3.10. Potassium formate

Potassium formate salts have several advantages in comparison to alcohols like methanol and ethanol for alkaline fuel cell applications. They are in solid state, so they can be stored and transported easily, and then later combined with water to obtain a liquid fuel solution. Although the industrial production still relies on fossil fuels, formic acid (potassium formate precursor) can also be produced by renewable means with electrochemical reduction or catalytic hydrogenation of CO<sub>2</sub>. The worldwide production of formic acid is estimated at  $7.2 \times 10^5 \text{ t y}^{-1}$ .<sup>223</sup> Potassium formate has a low toxicity and is a nonflammable, nonvolatile and noncorrosive fuel with a high theoretical voltage.<sup>224,225</sup>

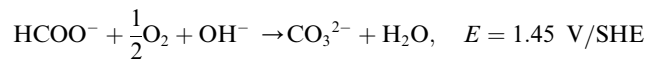
Anode:



Cathode:



Overall:<sup>223</sup>



Zeng *et al.*<sup>226</sup> report a single alkaline exchange membrane direct formate fuel cell (AEM DFFC) consisting of a carbon-supported palladium catalyst at the anode, a quaternised polysulfone membrane, and a non-precious Fe-CO catalyst at the cathode. It demonstrates that the AEM DFFC yields a peak power density of  $130 \text{ mW cm}^{-2}$  with 5 M potassium formate (HCOOK) at  $80 \text{ }^\circ\text{C}$ , and dry oxygen as the cathode feed. It is further shown that, with the addition of 1 M KOH to potassium formate, the peak power density rises to as high as  $250 \text{ mW cm}^{-2}$  at the same operating temperature and dry oxygen as the cathode feed. Miller *et al.*<sup>223</sup> developed a DFFC fed with 4 M potassium formate and 4 M KOH at  $60 \text{ }^\circ\text{C}$  and utilising humidified oxygen as the cathode feed. A power density of  $243 \text{ mW cm}^{-2}$  was achieved with a nanostructured Pd/C-CeO<sub>2</sub> anode catalyst and Fe-Co/C cathode catalyst. Nguyen *et al.*<sup>224</sup> demonstrated a Pt-free DFFC operating at ambient temperature employing an ACTA Hypermac 4020 Fe-Co second-generation cathode catalyst and Pd black anode catalyst with an A201 Tokuyama AEM. A DFFC fuelled with a 1 M HCOOK and 2 M KOH solution at the anode and oxygen at the cathode, produced a power density of  $35 \text{ mW cm}^{-2}$  at  $20 \text{ }^\circ\text{C}$ . When the same fuel cell was fed with only 1 M HCOOK at the anode, it produced a power density of  $18 \text{ mW cm}^{-2}$  at  $20 \text{ }^\circ\text{C}$ . Tran *et al.*<sup>227</sup> describe a fuel flexible alkaline direct liquid fuel cell fed with 1 M HCOOK and 2 M KOH at the anode and humidified oxygen as the cathode feed, which achieved a power density of  $302 \text{ mW cm}^{-2}$  at  $60 \text{ }^\circ\text{C}$ . The fuel cell employed an A201 Tokuyama AEM and Pd black anode catalyst and Pt black cathode catalyst. Bartrom *et al.*<sup>228</sup> investigated the performance of an alkaline DFFC employing an A201 Tokuyama AEM, which ran under the same conditions as reported by Tran *et al.*<sup>227</sup> and produced a power density of  $267 \text{ mW cm}^{-2}$  at  $60 \text{ }^\circ\text{C}$ . Jiang and Wieckowski<sup>225</sup> studied a DFFC with Pd anode and Ag cathode catalysts operating at intermediate temperature. Single cell measurements have shown increased performance with increasing temperature and increased formate concentrations. A DFFC operated with 6 M HCOOK produced a power density of around  $160 \text{ mW cm}^{-2}$  at  $120 \text{ }^\circ\text{C}$ , employing a polybenzimidazole-based AEM (FuMA-tTech GmBH).

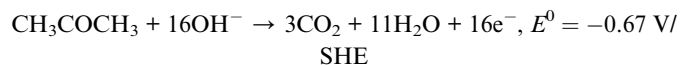
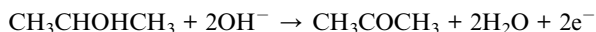
### 3.11. 2-Propanol

2-Propanol has several advantages for use as a fuel; relatively low toxicity, it is less prone to anode poisoning at low potentials, and it is less prone to crossover and cathode poisoning than methanol.<sup>229</sup> It is readily available as rubbing alcohol, but there is a significant concern with the use of 2-propanol as a fuel in

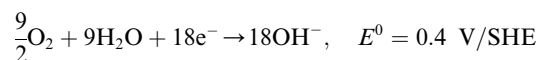


fuel cells, as it cannot oxidise to CO<sub>2</sub> completely (oxidation stops at acetone), meaning the concentration of acetone in the fuel compartment increases during the operation of the device. Catalysts highly resistant to acetone need to be chosen for such a fuel cell.<sup>227</sup>

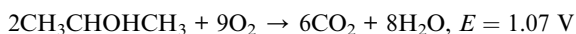
Anode:



Cathode:



Overall:<sup>182</sup>



Markiewicz and Bergens<sup>230</sup> developed a prototype alkaline direct 2-propanol fuel cell without a membrane; instead it used 5 M KOH as a liquid electrolyte. It was fuelled with 100% 2-propanol and oxygen with 0.1 MPa back-pressure and operated at 70 °C. A power density of 22.3 mW mg<sub>Pt</sub><sup>-1</sup> was achieved with Pt/C cathode and anode catalysts.

Also, a fuel flexible alkaline direct fuel cell was described by Tran *et al.*<sup>227</sup> and tested with different fuels. They have shown that a one catalyst combination can be used efficiently with different fuels in an alkaline fuel cell, a flexibility of choice of fuel which cannot be reached with an acidic fuel cell. At 60 °C the following maximum power densities were observed: ethanol 128 mW cm<sup>-2</sup>, 1-propanol 101 mW cm<sup>-2</sup>, 2-propanol 40 mW cm<sup>-2</sup>, ethylene glycol 117 mW cm<sup>-2</sup>, glycerol 78 mW cm<sup>-2</sup> and propylene glycol 75 mW cm<sup>-2</sup> (Pd black anode catalyst and Pt black cathode catalyst). All alcohol anode fuels consisted of 1 M alcohol with 2 M KOH, and oxygen was used as the cathode feed and the A201 Tokuyama as the AEM.

## 4. Summary and outlook

PEMs are already well established and produced commercially, the most noted example being the Nafion® PEM, but AEMs have not yet entered mass production.<sup>70,109</sup> Examples of commercial AEMs include the A201 membrane from Tokuyama Corporation (Japan), which utilises an unspecified polymer backbone, a Morgane ADP membrane from Solvay (Belgium), which is a cross-linked quaternary ammonium type AEM,<sup>231,232</sup> the FAA membrane from Fumatech (Germany) is a non-reinforced membrane based on polysulfones,<sup>70</sup> the Neosepta AHA from Tokuyama, a reinforced quaternary ammonium type AEM<sup>231</sup> and the Tokuyama A006 membrane.<sup>233</sup>

Currently, AEMFCs receive ever-increasing attention because of their overwhelming superiority compared with PEMFCs:

(a) Enhanced oxygen reduction and fuel (*i.e.* alcohols) oxidation catalysis in an alkaline environment, allowing for the use of less expensive, Pt-free or precious group metal-free catalysts such as (Ni, Co, Ru, *etc.*).<sup>18,234</sup>

(b) Extended range of cell and stack materials stable in the fuel cell environment; the reactive alkaline environment is less aggressive compared to the acidic environment in PEMFCs causing high corrosion.

(c) A wider choice of fuels (*i.e.* alcohols) in addition to pure hydrogen (mainly methanol and ethanol, polyols (glycerol, glucose, ethylene glycol), N-based fuels (hydrazine and ammonia)).

(d) A wider selection of less expensive polymers with good durability (fluorinated raw materials are not necessary).

(e) Reduced permeation of fuel through the AEMs; the OH<sup>-</sup> anionic current in AEMs has an opposite direction compared to the H<sup>+</sup> cationic current in PEMs, and, therefore, causes a reduced fuel crossover, due to the reverse direction of the electro-osmotic drag.<sup>13</sup>

There are several approaches of designing AEMs in terms of different backbone materials and functional groups. Among diverse backbone materials, the use of naturally derived materials is shown to have great potential, where the attachment of quaternary ammonium functional groups to the OH or NH<sub>2</sub> functional groups present on the polysaccharides *via* an ether linkage is a promising way of obtaining suitable AEMs.

The most appropriate and practical approach in characterising the potential of AEMs is the testing in actual AEMFCs, as the viewing of the AEM, electrocatalysts and their interfaces as a whole system rather than discrete components provides more accurate information about their suitability.<sup>235</sup> Characterisation of the newly developed AEMs should include a characterisation in a standard fuel cell system operating on a predetermined fuel with a predetermined standard concentration and the same alkali content under a fixed operating temperature. The MEA components should be unified regarding cathode and anode catalysts, as well as catalyst support materials. Only in such a way could different AEMs be compared regarding their applicability in AEMFCs. In this way, a direct comparison of newly developed AEMs could be performed, and the search for suitable AEM materials would be simplified. At present, a lot of uncertainty is present in this area, as it is hard to determine which is the predominant factor that affects the fuel cell performance, therefore, rushed assumptions can be made. This could mean a membrane could be marked unfit/fit based on its power density, which could be assumed wrongly, as the fault for low/high performance could lie in fuel cell operating conditions or other MEA materials. The testing of potential AEMs should include a test of the membrane in differently designed fuel cell set-ups if the AEM is thought to be more suitably embedded in a different MEA, or better performing under different operating conditions, and inclusion of different cathode and anode catalysts.

Another approach of determining the suitability of developed AEMs for fuel cell applications is measuring only the ion (*e.g.* OH<sup>-</sup>) conductivity of the AEM, which can also lead to false assumptions, as a high ion conductivity does not guarantee





a good fuel cell performance. The method should also be standardised if the method of hydroxide conductivity of AEMs should be used to determine suitable AEMs. It is also troubling to compare OH conductivity data among different AEMs, as they may be measured under humidified conditions, in pure water, or in alkaline solutions, and can, therefore, produce incomparable results. It is also important to note if the membranes are in their OH form (exchanged to hydroxide form from NaOH/KOH solutions), as then they are also partially contaminated with bicarbonate and carbonate anions, due to the reaction of OH<sup>-</sup> with CO<sub>2</sub> from the atmosphere during handling and testing. Therefore, the obtained hydroxide conductivities also depend on the degree of carbonation.<sup>235</sup> Other potential fuel cell operating limitations should also be noted and include an excessive water uptake, as a water uptake over 50% renders the membrane unusable in a fuel cell, even if it obtains a high hydroxide conductivity.

The research focus should include the development of highly alkaline stable AEMs, as the fuel cell should perform long term without deterioration of its performance. The AEMs are not the only components of AEMFCs that are susceptible to degradation, as the catalysts and the supporting layers can deteriorate. To identify the optimal catalysts and MEAs, a standard membrane (comparable to the Nafion PEM) should also be chosen and tested in a standardised AAEMFC fuel cell, which would then be used as a standard reference AEM.

## Conflicts of interest

There are no conflicts to declare.

## Abbreviations

|        |  |
|--------|--|
| AAEMFC | Alkaline anion exchange membrane fuel cell |
| AEM    | Anion exchange membrane                    |
| AEMFC  | Anion exchange membrane fuel cell          |
| BC     | Bacterial cellulose                        |
| CNC    | Nanocrystalline cellulose                  |
| CNF    | Nanofibrillar cellulose                    |
| CS     | Chitosan                                   |
| DAFC   | Direct alkaline fuel cell                  |
| DEFC   | Direct ethanol fuel cell                   |
| DFFC   | Direct formate fuel cell                   |
| DMFC   | Direct methanol fuel cell                  |
| DSC    | Differential scanning calorimetry          |
| EG     | Ethylene glycol                            |
| ETFE   | Ethylene tetrafluoroethylene               |
| GDL    | Gas diffusion layer                        |
| GO     | Graphene oxide                             |
| HOR    | Hydrogen oxidation reaction                |
| IEC    | Ion exchange capacity                      |
| MEA    | Membrane electrode assembly                |
| MPL    | Micro porous layer                         |
| ORR    | Oxygen reduction reaction                  |
| PBI    | Polybenzimidazole                          |
| PEEK   | Poly(ether ether ketone)                   |
| PEI    | Polyethyleneimine                          |

|       |                                    |
|-------|------------------------------------|
| PEKK  | Poly(ether ether ketone)           |
| PEM   | Proton exchange membrane           |
| PEMFC | Proton exchange membrane fuel cell |
| PPO   | Polyphenylene oxide                |
| PS    | Polystyrene                        |
| Pt    | Platinum                           |
| PTFE  | Polytetrafluoroethylene            |
| PVA   | Polyvinyl alcohol                  |
| PVBC  | Poly(vinylbenzyl chloride)         |
| TGA   | Thermogravimetric analysis         |

## Acknowledgements

The authors would like to acknowledge the financial support received in the frame of the Slovenian Research Agency Young Researcher Programme (P2-0118/0795), M-era.NET program (NanoEIEm – Designing new renewable nano-structured electrode and membrane materials for direct alkaline ethanol fuel cell - <http://nanoelmem.fs.um.si/>, Grant number C3330-17-500098), the Textile Chemistry Programme (P2-0118) and project “Graphene Oxide based MEAs for the Direct Ethanol Fuel Cell” (Grant number N2-0087).

## References

- B. G. Pollet, S. S. Kocha and I. Staffell, Current status of automotive fuel cells for sustainable transport, *Curr. Opin. Electrochem.*, 2019, **16**, 90–95, DOI: 10.1016/j.coelec.2019.04.021.
- A. Arshad, H. M. Ali, A. Habib, M. A. Bashir, M. Jabbar and Y. Yan, Energy and exergy analysis of fuel cells: A review, *Therm. Sci. Eng. Prog.*, 2019, **9**, 308–321, DOI: 10.1016/J.TSEP.2018.12.008.
- W. Gong, X. Yan, C. Hu, L. Wang and L. Gao, Fast and accurate parameter extraction for different types of fuel cells with decomposition and nature-inspired optimization method, *Energy Convers. Manage.*, 2018, **174**, 913–921, DOI: 10.1016/j.enconman.2018.08.082.
- R. Cownden, M. Nahon and M. A. Rosen, Exergy analysis of a fuel cell power system for transportation applications, *Int. J. Exergy*, 2001, **1**, 112–121, DOI: 10.1016/S1164-0235(01)00017-6.
- R. O'Hayre, S.-W. Cha, W. G. Colella and F. B. Prinz, *Fuel Cell Fundamentals*, John Wiley & Sons, 2016, DOI: 10.1017/CBO9781107415324.004.
- E. Bakangura, L. Wu, L. Ge, Z. Yang and T. Xu, Mixed matrix proton exchange membranes for fuel cells: State of the art and perspectives, *Prog. Polym. Sci.*, 2016, **57**, 103–152, DOI: 10.1016/j.progpolymsci.2015.11.004.
- A. Serov, I. V. Zenyuk, C. G. Arges and M. Chatenet, Hot topics in alkaline exchange membrane fuel cells, *J. Power Sources*, 2018, **375**, 149–157, DOI: 10.1016/j.jpowsour.2017.09.068.
- M. Kendall, Fuel cell development for New Energy Vehicles (NEVs) and clean air in China, *Prog. Nat. Sci.: Mater. Int.*, 2018, **28**, 113–120, DOI: 10.1016/j.pnsc.2018.03.001.



- 9 A. Kumar, T. Singh and S. Singh, A Comprehensive Review of Fuel Cell and its Types, *Int. J. Res. Mech. Eng. Technol.*, 2013, **5762**, 13–21.
- 10 X. Sun, Y. Li and M.-J. Li, Highly dispersed palladium nanoparticles on carbon-decorated porous nickel electrode: an effective strategy to boost direct ethanol fuel cell up to 202 mW cm<sup>-2</sup>, *ACS Sustainable Chem. Eng.*, 2019, **7**(13), 11186–11193, DOI: 10.1021/acssuschemeng.9b00355.
- 11 G. Merle, M. Wessling and K. Nijmeijer, Anion exchange membranes for alkaline fuel cells: A review, *J. Membr. Sci.*, 2011, **377**, 1–35, DOI: 10.1016/j.memsci.2011.04.043.
- 12 Z. F. Pan, R. Chen, L. An and Y. S. Li, Alkaline anion exchange membrane fuel cells for cogeneration of electricity and valuable chemicals, *J. Power Sources*, 2017, **365**, 430–445, DOI: 10.1016/j.jpowsour.2017.09.013.
- 13 J. Cheng, G. He and F. Zhang, A mini-review on anion exchange membranes for fuel cell applications: Stability issue and addressing strategies, *Int. J. Hydrogen Energy*, 2015, **40**, 7348–7360, DOI: 10.1016/j.ijhydene.2015.04.040.
- 14 D. R. Dekel, Review of cell performance in anion exchange membrane fuel cells, *J. Power Sources*, 2018, **375**, 158–169, DOI: 10.1016/j.jpowsour.2017.07.117.
- 15 X. Peng, D. Kulkarni, Y. Huang, T. J. Omasta, B. Ng, Y. Zheng, L. Wang, J. M. Lamanna, D. S. Hussey, J. R. Varcoe, I. V. Zenyuk and W. E. Mustain, Using operando techniques to understand and design high performance and stable alkaline membrane fuel cells, *Nat. Commun.*, 2020, 3561, DOI: 10.1038/s41467-020-17370-7.
- 16 C. Simon, D. Kartouzian, D. Müller, F. Wilhelm and H. A. Gasteiger, Impact of Microporous Layer Pore Properties on Liquid Water Transport in PEM Fuel Cells: Carbon Black Type and Perforation, *J. Electrochem. Soc.*, 2017, **164**, F1697–F1711, DOI: 10.1149/2.1321714jes.
- 17 R. B. Kaspar, M. P. Letterio, J. A. Wittkopf, K. Gong, S. Gu and Y. Yan, Manipulating Water in High-Performance Hydroxide Exchange Membrane Fuel Cells through Asymmetric Humidification and Wetproofing, *J. Electrochem. Soc.*, 2015, **162**, F483–F488, DOI: 10.1149/2.0131506jes.
- 18 M. Z. F. Kamarudin, S. K. Kamarudin, M. S. Masdar and W. R. W. Daud, Review: Direct ethanol fuel cells, *Int. J. Hydrogen Energy*, 2013, **38**, 9438–9453, DOI: 10.1016/j.ijhydene.2012.07.059.
- 19 S. Gottesfeld, D. R. Dekel, M. Page, C. Bae, Y. Yan, P. Zelenay and Y. S. Kim, Anion exchange membrane fuel cells: Current status and remaining challenges, *J. Power Sources*, 2018, **375**, 170–184, DOI: 10.1016/j.jpowsour.2017.08.010.
- 20 E. S. Davydova, S. Mukerjee, F. Jaouen and D. R. Dekel, Electrocatalysts for Hydrogen Oxidation Reaction in Alkaline Electrolytes, *ACS Catal.*, 2018, **8**, 6665–6690, DOI: 10.1021/acscatal.8b00689.
- 21 K. Elbert, J. Hu, Z. Ma, Y. Zhang, G. Chen, W. An, P. Liu, H. S. Isaacs, R. R. Adzic and J. X. Wang, Elucidating Hydrogen Oxidation/Evolution Kinetics in Base and Acid by Enhanced Activities at the Optimized Pt Shell Thickness on the Ru Core, *ACS Catal.*, 2015, **5**, 6764–6772, DOI: 10.1021/acscatal.5b01670.
- 22 E. G. Mahoney, W. Sheng, Y. Yan and J. G. Chen, Platinum-Modified Gold Electrocatalysts for the Hydrogen Oxidation Reaction in Alkaline Electrolytes, *ChemElectroChem*, 2014, **1**, 2058–2063, DOI: 10.1002/celec.201402159.
- 23 S. M. Alia, B. S. Pivovar and Y. Yan, Platinum-Coated Copper Nanowires with High Activity for Hydrogen Oxidation Reaction in Base, *J. Am. Chem. Soc.*, 2013, **135**, 13473–13478, DOI: 10.1021/ja405598a.
- 24 J. Zheng, S. Zhou, S. Gu, B. Xu and Y. Yan, Size-Dependent Hydrogen Oxidation and Evolution Activities on Supported Palladium Nanoparticles in Acid and Base, *J. Electrochem. Soc.*, 2016, **163**, F499–F506, DOI: 10.1149/2.0661606jes.
- 25 M. H. Martin and A. Lasia, Hydrogen sorption in Pd monolayers in alkaline solution, *Electrochim. Acta*, 2009, **54**, 5292–5299, DOI: 10.1016/J.ELECTACTA.2009.01.051.
- 26 S. Henning, J. Herranz and H. A. Gasteiger, Bulk-Palladium and Palladium-on-Gold Electrocatalysts for the Oxidation of Hydrogen in Alkaline Electrolyte, *J. Electrochem. Soc.*, 2015, **162**, F178–F189, DOI: 10.1149/2.1081501jes.
- 27 J. Durst, A. Siebel, C. Simon, F. Hasché, J. Herranz and H. A. Gasteiger, New insights into the electrochemical hydrogen oxidation and evolution reaction mechanism, *Energy Environ. Sci.*, 2014, **7**, 2255–2260, DOI: 10.1039/C4EE00440J.
- 28 M. Bellini, M. V. Pagliaro, A. Lenarda, P. Fornasiero, M. Marelli, C. Evangelisti, M. Innocenti, Q. Jia, S. Mukerjee, J. Jankovic, L. Wang, J. R. Varcoe, C. B. Krishnamurthy, I. Grinberg, E. Davydova, D. R. Dekel, H. A. Miller and F. Vizza, Palladium–Ceria Catalysts with Enhanced Alkaline Hydrogen Oxidation Activity for Anion Exchange Membrane Fuel Cells, *ACS Appl. Energy Mater.*, 2019, **2**, 4999–5008, DOI: 10.1021/acsaem.9b00657.
- 29 J. Ohyama, T. Sato, Y. Yamamoto, S. Arai and A. Satsuma, Size Specifically High Activity of Ru Nanoparticles for Hydrogen Oxidation Reaction in Alkaline Electrolyte, *J. Am. Chem. Soc.*, 2013, **135**, 8016–8021, DOI: 10.1021/ja4021638.
- 30 J. Zheng, Z. Zhuang, B. Xu and Y. Yan, Correlating Hydrogen Oxidation/Evolution Reaction Activity with the Minority Weak Hydrogen-Binding Sites on Ir/C Catalysts, *ACS Catal.*, 2015, **5**, 4449–4455, DOI: 10.1021/acscatal.5b00247.
- 31 M. A. Montero, M. R. G. de Chialvo and A. C. Chialvo, Evaluation of the kinetic parameters of the hydrogen oxidation reaction on nanostructured iridium electrodes in alkaline solution, *J. Electroanal. Chem.*, 2016, **767**, 153–159, DOI: 10.1016/J.JELECHEM.2016.02.024.
- 32 M. A. Montero, J. L. Fernández, M. R. Gennero de Chialvo and A. C. Chialvo, Characterization and kinetic study of a nanostructured rhodium electrode for the hydrogen oxidation reaction, *J. Power Sources*, 2014, **254**, 218–223, DOI: 10.1016/J.JPOWSOUR.2013.12.095.



- 33 D. Floner, C. Lamy and J.-M. Leger, Electrocatalytic oxidation of hydrogen on polycrystal and single-crystal nickel electrodes, *Surf. Sci.*, 1990, **234**, 87–97, DOI: 10.1016/0039-6028(90)90668-X.
- 34 S. Lu, J. Pan, A. Huang, L. Zhuang and J. Lu, Alkaline polymer electrolyte fuel cells completely free from noble metal catalysts, *Proc. Natl. Acad. Sci. U. S. A.*, 2008, **105**, 20611–20614, DOI: 10.1073/PNAS.0810041106.
- 35 Z. Zhuang, S. A. Giles, J. Zheng, G. R. Jenness, S. Caratzoulas, D. G. Vlachos and Y. Yan, Nickel supported on nitrogen-doped carbon nanotubes as hydrogen oxidation reaction catalyst in alkaline electrolyte, *Nat. Commun.*, 2016, **7**, 10141, DOI: 10.1038/ncomms10141.
- 36 W. Sheng, A. P. Bivens, M. Myint, Z. Zhuang, R. V. Forest, Q. Fang, J. G. Chen and Y. Yan, Non-precious metal electrocatalysts with high activity for hydrogen oxidation reaction in alkaline electrolytes, *Energy Environ. Sci.*, 2014, **7**, 1719–1724, DOI: 10.1039/C3EE43899F.
- 37 E. S. Davydova, F. D. Speck, M. T. Y. Paul, D. R. Dekel and S. Cherevko, Stability Limits of Ni-Based Hydrogen Oxidation Electrocatalysts for Anion Exchange Membrane Fuel Cells, *ACS Catal.*, 2019, **9**, 6837–6845, DOI: 10.1021/acscatal.9b01582.
- 38 E. H. Yu, U. Krewer and K. Scott, Principles and materials aspects of direct alkaline alcohol fuel cells, *Energies*, 2010, **3**, 1499–1528, DOI: 10.3390/en3081499.
- 39 A. Verma and S. Basu, Direct alkaline fuel cell for multiple liquid fuels: Anode electrode studies, *J. Power Sources*, 2007, **174**, 180–185, DOI: 10.1016/j.jpowsour.2007.07.077.
- 40 Y. Zhang, C. Wang, N. Wan and Z. Mao, Deposited RuO<sub>2</sub>-IrO<sub>2</sub>/Pt electrocatalyst for the regenerative fuel cell, *Int. J. Hydrogen Energy*, 2007, **32**(3), 400–404, DOI: 10.1016/j.ijhydene.2006.06.047.
- 41 C. Zhou, H. Wang, J. Liang, F. Peng, H. Yu and J. Yang, Effects of RuO<sub>2</sub> Content in Pt/RuO<sub>2</sub>/CNTs Nanocatalyst on the Electrocatalytic Oxidation Performance of Methanol, *Chin. J. Catal.*, 2008, **29**(11), 1093–1098, DOI: 10.1016/S1872-2067(09)60007-3.
- 42 T. Sakamoto, K. Asazawa, K. Yamada and H. Tanaka, Study of Pt-free anode catalysts for anion exchange membrane fuel cells, *Catal. Today*, 2011, **164**, 181–185, DOI: 10.1016/J.CATTOD.2010.11.012.
- 43 J. Sanabria-Chinchilla, K. Asazawa, T. Sakamoto, K. Yamada, H. Tanaka and P. Strasser, Noble metal-free hydrazine fuel cell catalysts: EPOC effect in competing chemical and electrochemical reaction pathways, *J. Am. Chem. Soc.*, 2011, **133**, 5425–5431, DOI: 10.1021/ja111160r.
- 44 R. Ghasemi, B. K. Moghadas and I. Mohammadi, Solvothermal synthesis of Pd<sub>10</sub>-Ni<sub>45</sub>-Co<sub>45</sub>/rGO composites as novel electrocatalysts for enhancement of the performance of DBFC, *Int. J. Hydrogen Energy*, 2020, **45**(41), 21808–21815, DOI: 10.1016/j.ijhydene.2020.05.172.
- 45 J. Guo, R. Chen, F. C. Zhu, S. G. Sun and H. M. Villullas, New understandings of ethanol oxidation reaction mechanism on Pd/C and Pd<sub>2</sub>Ru/C catalysts in alkaline direct ethanol fuel cells, *Appl. Catal., B*, 2018, **224**, 602–611, DOI: 10.1016/j.apcatb.2017.10.037.
- 46 H. Erikson, A. Sarapuu and K. Tammeveski, Oxygen Reduction Reaction on Silver Catalysts in Alkaline Media: a Minireview, *ChemElectroChem*, 2019, **6**, 73–86, DOI: 10.1002/celec.201800913.
- 47 J. S. Spendelov and A. Wieckowski, Electrocatalysis of oxygen reduction and small alcohol oxidation in alkaline media, *Phys. Chem. Chem. Phys.*, 2007, **9**, 2654–2675, DOI: 10.1039/b703315j.
- 48 M. M. Hossen, K. Artyushkova, P. Atanassov and A. Serov, Synthesis and characterization of high performing Fe–N–C catalyst for oxygen reduction reaction (ORR) in Alkaline Exchange Membrane Fuel Cells, *J. Power Sources*, 2018, **375**, 214–221, DOI: 10.1016/j.jpowsour.2017.08.036.
- 49 E. H. Yu, K. Scott and R. W. Reeve, Electrochemical Reduction of Oxygen on Carbon Supported Pt and Pt/Ru Fuel Cell Electrodes in Alkaline Solutions, *Fuel Cells*, 2003, **3**, 169–176, DOI: 10.1002/face.200330129.
- 50 J. Kim, T. Momma and T. Osaka, Cell performance of Pd–Sn catalyst in passive direct methanol alkaline fuel cell using anion exchange membrane, *J. Power Sources*, 2009, **189**, 999–1002, DOI: 10.1016/j.jpowsour.2008.12.108.
- 51 X. Y. Huang, A. J. Wang, L. Zhang, Q. L. Zhang, H. Huang and J. J. Feng, A simple wet-chemical strategy for facile fabrication of hierarchical PdAu nanodendrites as excellent electrocatalyst for oxygen reduction reaction, *J. Colloid Interface Sci.*, 2019, **552**, 51–58, DOI: 10.1016/j.jcis.2019.04.093.
- 52 H. Yin, S. Liu, C. Zhang, J. Bao, Y. Zheng, M. Han and Z. Dai, Well-coupled graphene and pd-based bimetallic nanocrystals nanocomposites for electrocatalytic oxygen reduction reaction, *ACS Appl. Mater. Interfaces*, 2014, **6**, 2086–2094, DOI: 10.1021/am405164f.
- 53 N. Todoroki and T. Wadayama, Oxygen reduction reaction activity for cobalt-deposited Pt(111) model catalyst surfaces in alkaline solution, *Electrochemistry*, 2018, **86**, 243–245, DOI: 10.5796/electrochemistry.18-00024.
- 54 F. H. B. Lima and E. A. Ticianelli, Oxygen electrocatalysis on ultra-thin porous coating rotating ring/disk platinum and platinum-cobalt electrodes in alkaline media, *Electrochim. Acta*, 2004, **49**, 4091–4099, DOI: 10.1016/j.electacta.2004.04.002.
- 55 H. T. Chung, J. H. Won and P. Zelenay, Active and stable carbon nanotube/nanoparticle composite electrocatalyst for oxygen reduction, *Nat. Commun.*, 2013, **4**, 1922, DOI: 10.1038/ncomms2944.
- 56 V. M. Truong, J. R. Tolchard, J. Svendby, M. Manikandan, H. A. Miller, S. Sunde, H. Yang, D. R. Dekel and A. O. Barnett, Platinum and platinum group metal-free catalysts for anion exchange membrane fuel cells, *Energies*, 2020, **13**, 1–21, DOI: 10.3390/en13030582.
- 57 X. Song and D. Zhang, Bimetallic Ag–Ni/C particles as cathode catalyst in AFCs (alkaline fuel cells), *Energy*, 2014, **70**, 223–230, DOI: 10.1016/j.energy.2014.03.116.
- 58 L. Liao, Y. M. Zhao, C. Xu, X. Y. Zhou, P. J. Wei and J. G. Liu, B, N-codoped Cu–N/B–C Composite as an Efficient



- Electrocatalyst for Oxygen-Reduction Reaction in Alkaline Media, *ChemistrySelect*, 2020, 5, 3647–3654, DOI: 10.1002/slt.202000523.
- 59 R. Borup, J. Meyers, B. Pivovar, Y. S. Kim, R. Mukundan, N. Garland, D. Myers, M. Wilson, F. Garzon, D. Wood, P. Zelenay, K. More, K. Stroh, T. Zawodzinski, J. Boncella, J. E. McGrath, M. Inaba, K. Miyatake, M. Hori, K. Ota, Z. Ogumi, S. Miyata, A. Nishikata, Z. Siroma, Y. Uchimoto, K. Yasuda, K. Kimijima and N. Iwashita, Scientific Aspects of Polymer Electrolyte Fuel Cell Durability and Degradation, *Chem. Rev.*, 2007, 107(10), 3904–3951, DOI: 10.1021/cr050182l.
- 60 M. Bandapati, S. Goel and B. Krishnamurthy, Platinum utilization in proton exchange membrane fuel cell and direct methanol fuel cell, *J. Electrochem. Sci. Eng.*, 2019, 9(4), 281–310, DOI: 10.5599/jese.665.
- 61 S. Samad, K. S. Loh, W. Y. Wong, T. K. Lee, J. Sunarso, S. T. Chong and W. R. W. Daud, Carbon and non-carbon support materials for platinum-based catalysts in fuel cells, *Int. J. Hydrogen Energy*, 2018, 43(16), 7823–7854, DOI: 10.1016/j.ijhydene.2018.02.154.
- 62 E. Antolini and E. R. Gonzalez, Ceramic materials as supports for low-temperature fuel cell catalysts, *Solid State Ionics*, 2009, 180, 746–763, DOI: 10.1016/j.ssi.2009.03.007.
- 63 K. N. Grew and W. K. S. Chiu, A Dusty Fluid Model for Predicting Hydroxyl Anion Conductivity in Alkaline Anion Exchange Membranes, *J. Electrochem. Soc.*, 2010, 157, B327, DOI: 10.1149/1.3273200.
- 64 S. Maurya, S. H. Shin, Y. Kim and S. H. Moon, A review on recent developments of anion exchange membranes for fuel cells and redox flow batteries, *RSC Adv.*, 2015, 5, 37206–37230, DOI: 10.1039/c5ra04741b.
- 65 B. Cermenek, J. Ranninger and V. Hacker, *Alkaline Direct Ethanol Fuel Cell*, Elsevier Inc., 2019, DOI: 10.1016/B978-0-12-811458-2.00015-8.
- 66 J. Pan, C. Chen, Y. Li, L. Wang, L. Tan, G. Li, X. Tang, L. Xiao, J. Lu and L. Zhuang, Constructing ionic highway in alkaline polymer electrolytes, *Energy Environ. Sci.*, 2014, 7, 354–360, DOI: 10.1039/c3ee43275k.
- 67 N. Tanaka, M. Nagase and M. Higa, Preparation of aliphatic-hydrocarbon-based anion-exchange membranes and their anti-organic-fouling properties, *J. Membr. Sci.*, 2011, 384(1–2), 27–36, DOI: 10.1016/j.memsci.2011.08.064.
- 68 Z. Hu, W. Tang, D. Ning, X. Zhang, H. Bi and S. Chen, Fluorenyl-containing Quaternary Ammonium Poly(arylene ether sulfone)s for Anion Exchange Membrane Applications, *Fuel Cells*, 2016, 16(5), 557–567, DOI: 10.1002/fuce.201600015.
- 69 K. Wang, Q. Wu, X. Yan, J. Liu, L. Gao, L. Hu, N. Zhang, Y. Pan, W. Zheng and G. He, Branched poly(ether ether ketone) based anion exchange membrane for H<sub>2</sub>/O<sub>2</sub> fuel cell, *Int. J. Hydrogen Energy*, 2019, 44(42), 23750–23761, DOI: 10.1016/j.ijhydene.2019.07.080.
- 70 B. Kaker, S. Hribernik, T. Mohan, R. Kargl, K. Stana Kleinschek, E. Pavlica, A. Kreta, G. Bratina, S. J. Lue and M. Božič, Novel Chitosan–Mg(OH)<sub>2</sub>-Based Nanocomposite Membranes for Direct Alkaline Ethanol Fuel Cells, *ACS Sustainable Chem. Eng.*, 2019, 7, 19356–19368, DOI: 10.1021/acssuschemeng.9b02888.
- 71 B. P. Tripathi, M. Kumar and V. K. Shahi, Organic-inorganic hybrid alkaline membranes by epoxide ring opening for direct methanol fuel cell applications, *J. Membr. Sci.*, 2010, 360, 90–101, DOI: 10.1016/j.memsci.2010.05.005.
- 72 A. Zafar, A. Munsur, I. Hossain and S. Yong, Quaternary ammonium-functionalized hexyl bis(quaternary ammonium)-mediated partially crosslinked SEBSs as highly conductive and stable anion exchange membranes, *Int. J. Hydrogen Energy*, 2020, 45, 15658–15671, DOI: 10.1016/j.ijhydene.2020.04.063.
- 73 C. Zhang, J. Hu, J. Cong, Y. Zhao, W. Shen and H. Toyoda, Pulsed plasma-polymerized alkaline anion-exchange membranes for potential application in direct alcohol fuel cells, *J. Power Sources*, 2011, 196, 5386–5393, DOI: 10.1016/j.jpowsour.2011.02.073.
- 74 T. Yang, T. Ho, V. Vijayakumar, K. Kim and S. Yong, Anion exchange composite membranes composed of poly(phenylene oxide) containing quaternary ammonium and polyethylene support for alkaline anion exchange membrane fuel cell applications, *Solid State Ionics*, 2020, 344, 115153, DOI: 10.1016/j.ssi.2019.115153.
- 75 M. Nobuyo, K. Yamaguchi, K. Machida, T. Mori, and K. Yoshida, Alkaline electrolyte type formaldehyde fuel cells, Jpn. Kokai Tokkyo Koho, JP 63218165 A, 1988.
- 76 S. E. Stone C, A. E. Steck and B. Choudhury, Graft polymeric membranes, for e.g. ion-exchange membranes used in e.g. an electrochemical fuel cell, comprises one or more trifluorovinyl aromatic monomers, radiation graft polymerized to a polymeric base film, WO200158576-A1, AU200034134-A, EP1257348-A1, JP2003522224-W, EP1257348-B1, DE60014713-E, DE60014713-T2, CA2398836-C, 2000.
- 77 T. N. Danks, R. C. T. Slade and J. R. Varcoe, Comparison of PVDF- and FEP-based radiation-grafted alkaline anion-exchange membranes for use in low temperature portable DMFCs, *J. Mater. Chem.*, 2002, 12, 3371–3373, DOI: 10.1039/b208627a.
- 78 L. Li and Y. Wang, Quaternized polyethersulfone Cardo anion exchange membranes for direct methanol alkaline fuel cells, *J. Membr. Sci.*, 2005, 262(1–2), 1–4, DOI: 10.1016/j.memsci.2005.07.009.
- 79 J. R. Varcoe and R. C. T. Slade, An electron-beam-grafted ETFE alkaline anion-exchange membrane in metal-cation-free solid-state alkaline fuel cells, *Electrochem. Commun.*, 2006, 8(5), 839–843, DOI: 10.1016/j.elecom.2006.03.027.
- 80 X. Tan, Z. Sun, J. Pan, J. Zhao, H. Cao and H. Zhu, Alkaline stable pyrrolidinium-type main-chain polymer: The synergetic effect between adjacent cations, *J. Membr. Sci.*, 2021, 618, 118689.
- 81 C. Cheng, X. He, S. Huang, F. Zhang, Y. Guo, Y. Wen, B. Wu and D. Chen, Novel self-cross-linked multi-imidazolium cations long flexible side chains triblock copolymer anion exchange membrane based on ROMP-type polybenzonorborene, *Int. J. Hydrogen Energy*, 2020, 45(38), 19676–19690, DOI: 10.1016/j.ijhydene.2020.04.276.



- 82 Z. Wang, Z. Li, N. Chen, C. Lu, F. Wang and H. Zhu, Crosslinked poly(2,6-dimethyl-1,4-phenylene oxide) polyelectrolyte enhanced with poly(styrene-*b*-(ethylene-*co*-butylene)-*b*-styrene) for anion exchange membrane applications, *J. Membr. Sci.*, 2018, **564**, 492–500, DOI: 10.1016/j.memsci.2018.07.039.
- 83 L. Zhu, J. Pan, Y. Wang, J. Han, L. Zhuang and M. A. Hickner, Multication Side Chain Anion Exchange Membranes, *Macromolecules*, 2016, **49**, 815–824, DOI: 10.1021/acs.macromol.5b02671.
- 84 L. Li, J. Zhang, T. Jiang, X. Sun, Y. Li, X. Li, S. Yang, S. Lu, H. Wei and Y. Ding, High Ion Conductivity and Diffusivity in the Anion Exchange Membrane Enabled by Tethering with Multication Strings on the Poly(biphenyl alkylene) Backbone, *ACS Appl. Energy Mater.*, 2020, **3**(7), 6268–6279, DOI: 10.1021/acsaem.0c00409.
- 85 J. S. Olsson, T. H. Pham and P. Jannasch, Poly(arylene piperidinium) Hydroxide Ion Exchange Membranes: Synthesis, Alkaline Stability, and Conductivity, *Adv. Funct. Mater.*, 2018, **28**, 1702758, DOI: 10.1002/adfm.201702758.
- 86 J. S. Olsson, T. H. Pham and P. Jannasch, Tuning poly(arylene piperidinium) anion-exchange membranes by copolymerization, partial quaternization and crosslinking, *J. Membr. Sci.*, 2019, **578**, 183–195, DOI: 10.1016/j.memsci.2019.01.036.
- 87 J. Wang, Y. Zhao, B. P. Setzler, S. Rojas-carbonell, C. Ben Yehuda, A. Amel, M. Page, L. Wang, K. Hu, L. Shi, S. Gottesfeld, B. Xu and Y. Yan, Poly(aryl piperidinium) membranes and ionomers for hydroxide exchange membrane fuel cells, *Nat. Energy*, 2019, **4**, 392–398, DOI: 10.1038/s41560-019-0372-8.
- 88 Z. Zhang, X. Xiao, X. Yan, X. Liang and L. Wu, Highly conductive anion exchange membranes based on one-step benzylation modification of poly(ether ether ketone), *J. Membr. Sci.*, 2019, **574**, 205–211, DOI: 10.1016/j.memsci.2018.12.080.
- 89 M. Xu, M. Gang, L. Cao, X. He, Y. Song, Z. Jiang, H. Wu and Y. Su, Enhanced hydroxide ion conductivity of imidazolium functionalized poly(ether ether ketone) membrane by incorporating *N,N,N',N'*-tetramethyl-1,4-phenylenediamine, *Solid State Ionics*, 2018, **325**, 163–169, DOI: 10.1016/j.ssi.2018.08.009.
- 90 T. Li, X. Wu, W. Chen, X. Yan, D. Zhen, X. Gong, J. Liu, S. Zhang and G. He, Poly(ether ether ketone) based imidazolium as anion exchange membranes for alkaline fuel cells, *Chin. J. Chem. Eng.*, 2018, **26**, 2130–2138, DOI: 10.1016/j.cjche.2018.05.015.
- 91 A. L. G. Biancolli, D. Herranz, L. Wang, G. Stehlíková, R. Bance-Soualhi, J. Ponce-González, P. Ocón, E. A. Ticianelli, D. K. Whelligan, J. R. Varcoe and E. I. Santiago, ETFE-based anion-exchange membrane ionomer powders for alkaline membrane fuel cells: A first performance comparison of head-group chemistry, *J. Mater. Chem. A*, 2018, **6**, 24330–24341, DOI: 10.1039/c8ta08309f.
- 92 T. Hamada, K. Yoshimura, A. Hiroki and Y. Maekawa, Synthesis and characterization of aniline-containing anion-conducting polymer electrolyte membranes by radiation-induced graft polymerization, *J. Appl. Polym. Sci.*, 2018, **135**, 1–11, DOI: 10.1002/app.46886.
- 93 J. Ponce-González, D. K. Whelligan, L. Wang, R. Bance-Soualhi, Y. Wang, Y. Peng, H. Peng, D. C. Apperley, H. N. Sarode, T. P. Pandey, A. G. Divekar, S. Seifert, A. M. Herring, L. Zhuang and J. R. Varcoe, High performance aliphatic-heterocyclic benzyl-quaternary ammonium radiation-grafted anion-exchange membranes, *Energy Environ. Sci.*, 2016, **9**, 3724–3735, DOI: 10.1039/C6EE01958G.
- 94 K. Yoshimura, A. Hiroki, H. C. Yu, Y. Zhao, H. Shishitani, S. Yamaguchi, H. Tanaka and Y. Maekawa, Alkaline durable 2-methylimidazolium containing anion-conducting electrolyte membranes synthesized by radiation-induced grafting for direct hydrazine hydrate fuel cells, *J. Membr. Sci.*, 2019, **573**, 403–410, DOI: 10.1016/j.memsci.2018.12.002.
- 95 X. Zhang, X. Chu, M. Zhang, M. Zhu, Y. Huang, Y. Wang, L. Liu and N. Li, Molecularly designed, solvent processable tetraalkylammonium-functionalized fluoropolyolefin for durable anion exchange membrane fuel cells, *J. Membr. Sci.*, 2019, **574**, 212–221, DOI: 10.1016/j.memsci.2018.12.082.
- 96 L. Zhu, X. Peng, S. Shang, M. T. Kwasny, T. J. Zimudzi, X. Yu, N. Saikia, J. Pan, Z. Liu, G. N. Tew, W. E. Mustain, M. Yandrasits and M. A. Hickner, High Performance Anion Exchange Membrane Fuel Cells Enabled by Fluoropoly(olefin) Membranes, *Adv. Funct. Mater.*, 2019, 1902059, DOI: 10.1002/adfm.201902059.
- 97 L. Zhu, X. Yu, X. Peng, T. J. Zimudzi, N. Saikia, M. T. Kwasny, S. Song, D. I. Kushner, Z. Fu, G. N. Tew, W. E. Mustain, M. A. Yandrasits and M. A. Hickner, Poly(olefin)-Based Anion Exchange Membranes Prepared Using Ziegler–Natta Polymerization, *Macromolecules*, 2019, **52**, 4030–4041, DOI: 10.1021/acs.macromol.8b02756.
- 98 C. Yang, L. Liu, Y. Huang, J. Dong and N. Li, Anion-conductive poly(2,6-dimethyl-1,4-phenylene oxide) grafted with tailored polystyrene chains for alkaline fuel cells, *J. Membr. Sci.*, 2019, **573**, 247–256, DOI: 10.1016/j.memsci.2018.12.013.
- 99 H. Lim, B. Lee, D. Yun, A. Z. Al Munsur, J. E. Chae, S. Y. Lee, H. J. Kim, S. Y. Nam, C. H. Park and T. H. Kim, Poly(2,6-dimethyl-1,4-phenylene oxide)s with Various Head Groups: Effect of Head Groups on the Properties of Anion Exchange Membranes, *ACS Appl. Mater. Interfaces*, 2018, **10**, 41279–41292, DOI: 10.1021/acsami.8b13016.
- 100 G. Shukla and V. K. Shahi, Well-designed mono- and di-functionalized comb-shaped poly(2,6-dimethylphenylene oxide) based alkaline stable anion exchange membrane for fuel cells, *Int. J. Hydrogen Energy*, 2018, **43**, 21742–21749, DOI: 10.1016/j.ijhydene.2018.04.027.
- 101 Y. Zhu, L. Ding, X. Liang, M. A. Shehzad, L. Wang, X. Ge, Y. He, L. Wu, J. R. Varcoe and T. Xu, Beneficial use of rotatable-spacer side-chains in alkaline anion exchange membranes for fuel cells, *Energy Environ. Sci.*, 2018, **11**, 3472–3479, DOI: 10.1039/c8ee02071j.



- 102 X. Lin, J. R. Varcoe, S. D. Poynton, X. Liang, A. L. Ong, J. Ran, Y. Li and T. Xu, Alkaline polymer electrolytes containing pendant dimethylimidazolium groups for alkaline membrane fuel cells, *J. Mater. Chem. A*, 2013, **1**, 7262–7269, DOI: 10.1039/c3ta10308k.
- 103 Y. Xiao, W. Huang, K. Xu, M. Li, M. Fan and K. Wang, Preparation of anion exchange membrane with branch polyethyleneimine as main skeleton component, *Mater. Des.*, 2018, **160**, 698–707, DOI: 10.1016/j.matdes.2018.09.047.
- 104 C. Qu, H. Zhang, F. Zhang and B. Liu, A high-performance anion exchange membrane based on bi-guanidinium bridged polysilsesquioxane for alkaline fuel cell application, *J. Mater. Chem.*, 2012, **22**, 8203–8207, DOI: 10.1039/c2jm16211c.
- 105 Y. Yang, J. Wang, J. Zheng, S. Li and S. Zhang, A stable anion exchange membrane based on imidazolium salt for alkaline fuel cell, *J. Membr. Sci.*, 2014, **467**, 48–55, DOI: 10.1016/j.memsci.2014.05.017.
- 106 S. Yu, X. Ma, H. Liu and J. Hao, Highly stable double crosslinked membrane based on poly(vinylbenzyl chloride) for anion exchange membrane fuel cell, *Polym. Bull.*, 2018, **75**, 5163–5177, DOI: 10.1007/s00289-018-2312-3.
- 107 B. Qiu, B. Lin, L. Qiu and F. Yan, Alkaline imidazolium- and quaternary ammonium-functionalized anion exchange membranes for alkaline fuel cell applications, *J. Mater. Chem.*, 2012, **22**, 1040–1045, DOI: 10.1039/c1jm14331j.
- 108 Z. Zakaria, S. K. Kamarudin and S. N. Timmiati, Membranes for direct ethanol fuel cells: An overview, *Appl. Energy*, 2016, **163**, 334–342, DOI: 10.1016/j.apenergy.2015.10.124.
- 109 R. Vinodh, *Anion exchange membrane and its composites for fuel cell applications*, Anna University, 2012.
- 110 V. Vijayakumar and S. Y. Nam, Recent advancements in applications of alkaline anion exchange membranes for polymer electrolyte fuel cells, *J. Ind. Eng. Chem.*, 2018, **70**, 70–86, DOI: 10.1016/J.JIEC.2018.10.026.
- 111 Y. Wan, B. Peppley, K. A. M. Creber, V. T. Bui and E. Halliop, Quaternized-chitosan membranes for possible applications in alkaline fuel cells, *J. Power Sources*, 2008, **185**(1), 183–187, DOI: 10.1016/j.jpowsour.2008.07.002.
- 112 Y. Wan, K. A. M. Creber, B. Peppley and V. T. Bui, Ionic conductivity of chitosan membranes, *Polymer*, 2003, **44**, 1057–1065, DOI: 10.1016/S0032-3861(02)00881-9.
- 113 Y. Wan, K. A. M. Creber, B. Peppley and V. T. Bui, Ionic conductivity and related properties of crosslinked chitosan membranes, *J. Appl. Polym. Sci.*, 2003, **89**, 306–317, DOI: 10.1002/app.12090.
- 114 Y. Wan, K. A. M. Creber, B. Peppley, V. Tam Bui and E. Halliop, New solid polymer electrolyte membranes for alkaline fuel cells, *Polym. Int.*, 2005, **54**, 5–10, DOI: 10.1002/pi.1717.
- 115 Y. Wan, K. A. M. Creber, B. Peppley and V. T. Bui, Chitosan-based electrolyte composite membranes: II. Mechanical properties and ionic conductivity, *J. Membr. Sci.*, 2006, **284**, 331–338, DOI: 10.1016/j.memsci.2006.07.046.
- 116 Y. Wan, B. Peppley, K. A. M. Creber, V. T. Bui and E. Halliop, Preliminary evaluation of an alkaline chitosan-based membrane fuel cell, *J. Power Sources*, 2006, **162**(1), 105–113, DOI: 10.1016/j.jpowsour.2006.07.027.
- 117 Y. Wan, B. Peppley, K. A. M. Creber and V. T. Bui, Anion-exchange membranes composed of quaternized-chitosan derivatives for alkaline fuel cells, *J. Power Sources*, 2010, **195**(12), 3785–3793, DOI: 10.1016/j.jpowsour.2009.11.123.
- 118 J. Wang and L. Wang, Preparation and properties of organic–inorganic alkaline hybrid membranes for direct methanol fuel cell application, *Solid State Ionics*, 2014, **255**, 96–103, DOI: 10.1016/j.ssi.2013.12.013.
- 119 T. Zhou, X. He, F. Song and K. Xie, Chitosan Modified by Polymeric Reactive Dyes Containing Quaternary Ammonium Groups as a Novel Anion Exchange Membrane for Alkaline Fuel Cells, *Int. J. Electrochem. Sci.*, 2016, **11**, 590–608.
- 120 B. Wang, Y. Zhu, T. Zhou and K. Xie, ScienceDirect Synthesis and properties of chitosan membranes modified by reactive cationic dyes as a novel alkaline exchange membrane for low temperature fuel cells, *Int. J. Hydrogen Energy*, 2016, **41**, 18166–18177, DOI: 10.1016/j.ijhydene.2016.07.069.
- 121 T. Zhou, X. He and Z. Lu, Studies on a novel anion-exchange membrane based on chitosan and ionized organic compounds with multiwalled carbon nanotubes for alkaline fuel cells, *J. Appl. Polym. Sci.*, 2018, **135**, 1–11, DOI: 10.1002/app.46323.
- 122 L. Wang and B. Shi, Hydroxide Conduction Enhancement of Chitosan Membranes by Functionalized MXene, *Materials*, 2018, **11**, 2335, DOI: 10.3390/ma11112335.
- 123 L. Garcia-Cruz, C. Casado-Coterillo, J. Iniesta, V. Montiel and Á. Irabien, Preparation and characterization of novel chitosan-based mixed matrix membranes resistant in alkaline media, *J. Appl. Polym. Sci.*, 2015, **132**, 1–10, DOI: 10.1002/app.42240.
- 124 L. Liu and G. Sun, Simultaneously enhanced conductivity and dimensional stability of AAEM by crosslinked polymer microsphere with dense carrier sites, *J. Appl. Polym. Sci.*, 2018, **135**, 1–12, DOI: 10.1002/app.46715.
- 125 X. Zheng, C. Shang, J. Yang, J. Wang and L. Wang, Preparation and characterization of chitosan-crown ether membranes for alkaline fuel cells, *Synth. Met.*, 2019, **247**, 109–115, DOI: 10.1016/j.synthmet.2018.11.014.
- 126 Y. Wan, K. A. M. Creber, B. Peppley and V. T. Bui, Synthesis, Characterization and Ionic Conductive Properties of Phosphorylated Chitosan Membranes, *Macromol. Chem. Phys.*, 2003, **204**, 850–858.
- 127 J. Wang, R. He and Q. Che, Anion exchange membranes based on semi-interpenetrating polymer network of quaternized chitosan and polystyrene, *J. Colloid Interface Sci.*, 2011, **361**, 219–225, DOI: 10.1016/j.jcis.2011.05.039.
- 128 J. L. Wang, Q. T. Che and R. H. He, Chitosan for Anion Exchange Membranes Positively Charged Polystyrene Blended Quaternized Positively Charged Polystyrene Blended Quaternized Chitosan for Anion Exchange



- Membranes, *J. Electrochem. Soc.*, 2013, **160**, 168–174, DOI: 10.1149/2.080302jes.
- 129 J. Wang and R. He, Formation and evaluation of interpenetrating networks of anion exchange membranes based on quaternized chitosan and copolymer poly(acrylamide)/polystyrene, *Solid State Ionics*, 2015, **278**, 49–57, DOI: 10.1016/j.ssi.2015.05.017.
- 130 Y. Xiong, Q. L. Liu, Q. G. Zhang and A. M. Zhu, Synthesis and characterization of cross-linked quaternized poly(vinyl alcohol)/chitosan composite anion exchange membranes for fuel cells, *J. Power Sources*, 2008, **183**, 447–453.
- 131 J. Ming Yang and H. Chih Chiu, Preparation and characterization of polyvinyl alcohol/chitosan blended membrane for alkaline direct methanol fuel cells, *J. Membr. Sci.*, 2012, **419–420**, 65–71, DOI: 10.1016/j.memsci.2012.06.051.
- 132 G. M. Liao, C. C. Yang, C. C. Hu, Y. L. Pai and S. J. Lue, Novel quaternized polyvinyl alcohol/quaternized chitosan nanocomposite as an effective hydroxide-conducting electrolyte, *J. Membr. Sci.*, 2015, **485**, 17–29, DOI: 10.1016/j.memsci.2015.02.043.
- 133 X. Jiang, Y. Sun, H. Zhang and L. Hou, Preparation and characterization of quaternized poly(vinyl alcohol)/chitosan/MoS<sub>2</sub> composite anion exchange membranes with high selectivity, *Carbohydr. Polym.*, 2018, **180**, 96–103, DOI: 10.1016/j.carbpol.2017.10.023.
- 134 P. C. Li, G. M. Liao, S. R. Kumar, C. M. Shih, C. C. Yang, D. M. Wang and S. J. Lue, Fabrication and Characterization of Chitosan Nanoparticle-Incorporated Quaternized Poly(Vinyl Alcohol) Composite Membranes as Solid Electrolytes for Direct Methanol Alkaline Fuel Cells, *Electrochim. Acta*, 2016, **187**, 616–628, DOI: 10.1016/j.electacta.2015.11.117.
- 135 B. Feketeoldi and B. Cermenek, Chitosan-Based Anion Exchange Membranes for Direct Ethanol Fuel Cells, *J. Membr. Sci. Technol.*, 2016, **6**, 1–9, DOI: 10.4172/2155-9589.1000145.
- 136 J. M. Yang, C. S. Fan, N. C. Wang and Y. H. Chang, Evaluation of membrane preparation method on the performance of alkaline polymer electrolyte: Comparison between poly(vinyl alcohol)/chitosan blended membrane and poly(vinyl alcohol)/chitosan electrospun nanofiber composite membranes, *Electrochim. Acta*, 2018, **266**, 332–340, DOI: 10.1016/j.electacta.2018.02.043.
- 137 J. M. Yang and S. A. Wang, Preparation of graphene-based poly(vinyl alcohol)/chitosan nanocomposites membrane for alkaline solid electrolytes membrane, *J. Membr. Sci.*, 2015, **477**, 49–57, DOI: 10.1016/j.memsci.2014.12.028.
- 138 L. L. Wang, J. L. Wang, Y. Zhang and R. J. Feng, Alkaline hybrid composite membrane for direct methanol fuel cells application, *J. Electroanal. Chem.*, 2015, **759**, 174–183, DOI: 10.1016/j.jelechem.2015.11.012.
- 139 X. Cheng, J. Wang, Y. Liao, C. Li and Z. Wei, Enhanced Conductivity of Anion-Exchange Membrane by Incorporation of Quaternized Cellulose Nanocrystal, *ACS Appl. Mater. Interfaces*, 2018, **10**, 23774–23782, DOI: 10.1021/acsami.8b05298.
- 140 M. Rinaudo, Chitin and chitosan: Properties and applications, *Prog. Polym. Sci.*, 2006, **31**, 603–632, DOI: 10.1016/j.progpolymsci.2006.06.001.
- 141 S. Gorgieva, R. Vogrinčić and V. Kokol, Polydispersity and assembling phenomena of native and reactive dye-labelled nanocellulose, *Cellulose*, 2015, **22**, 3541–3558, DOI: 10.1007/s10570-015-0755-3.
- 142 P. Phanthong, P. Reubroycharoen, X. Hao, G. Xu, A. Abudula and G. Guan, Nanocellulose: Extraction and application, *Carbon Resour. Convers.*, 2018, **1**, 32–43, DOI: 10.1016/j.crcon.2018.05.004.
- 143 S. Gorgieva and J. Trček, Bacterial cellulose: Production, Modification and Perspectives in Biomedical Applications, *Nanomaterials*, 2019, **9**(10), 1352, DOI: 10.3390/nano9101352.
- 144 S. Gorgieva, Bacterial Cellulose as a Versatile Platform for Research and Development of Biomedical Materials, *Processes*, 2020, **8**, 624, DOI: 10.3390/pr8050624.
- 145 A. F. Martins, S. P. Facchi, H. D. M. Follmann, A. G. B. Pereira, A. F. Rubira and E. C. Muniz, Antimicrobial activity of chitosan derivatives containing N-quaternized moieties in its backbone: A review, *Int. J. Mol. Sci.*, 2014, **15**, 20800–20832, DOI: 10.3390/ijms151120800.
- 146 Y. Xiong, Q. L. Liu, Q. G. Zhang and A. M. Zhu, Synthesis and characterization of cross-linked quaternized poly(vinyl alcohol)/chitosan composite anion exchange membranes for fuel cells, *J. Power Sources*, 2008, **183**(2), 447–453, DOI: 10.1016/j.jpowsour.2008.06.004.
- 147 F. Luan, L. Wei, J. Zhang, W. Tan, Y. Chen, F. Dong, Q. Li and Z. Guo, Preparation and Characterization of Quaternized Chitosan Derivatives and Assessment of Their Antioxidant Activity, *Molecules*, 2018, **23**(3), 516, DOI: 10.3390/molecules23030516.
- 148 E. A. Stepnova, V. E. Tikhonov, T. A. Babushkina, T. P. Klimova, E. V. Vorontsov, V. G. Babak, S. A. Lopatin and I. A. Yamskov, New approach to the quaternization of chitosan and its amphiphilic derivatives, *Eur. Polym. J.*, 2007, **43**(6), 2414–2421, DOI: 10.1016/j.eurpolymj.2007.02.028.
- 149 K. Chen and S. Zeng, Preparation and Characterization of Quaternized Chitosan Coated Alginate Microspheres for Blue Dextran Delivery, *Polymers*, 2017, **9**(6), 210, DOI: 10.3390/polym9060210.
- 150 L. Wei, Q. Li, W. Tan, F. Dong, F. Luan and Z. Guo, Synthesis, Characterization, and the Antioxidant Activity of Double Quaternized Chitosan Derivatives, *Molecules*, 2017, **22**(3), 501, DOI: 10.3390/molecules22030501.
- 151 A. P. Abbott, T. J. Bell, S. Handa and B. Stoddart, Cationic functionalisation of cellulose using a choline based ionic liquid analogue, *Green Chem.*, 2006, **8**, 784–786, DOI: 10.1039/b605258d.
- 152 T. Józwiak, U. Filipkowska, P. Szymczyk, J. Rodziewicz and A. Mielcarek, Effect of ionic and covalent crosslinking agents on properties of chitosan beads and sorption



- effectiveness of Reactive Black 5 dye, *React. Funct. Polym.*, 2017, **114**, 58–74, DOI: 10.1016/j.reactfunctpolym.2017.03.007.
- 153 J. Runhong, L. H. Hsu, E. S. Xiao, X. Guo and Y. Zhang, Using genipin as a “green” crosslinker to fabricate chitosan membranes for pervaporative dehydration of isopropanol, *Sep. Purif. Technol.*, 2020, **244**, 116843, DOI: 10.1016/j.seppur.2020.116843.
- 154 S. Gorgieva, T. Vuherer and V. Kokol, Autofluorescence-aided assessment of integration and  $\mu$ -structuring in chitosan/gelatin bilayer membranes with rapidly mineralized interface in relevance to guided tissue regeneration, *Mater. Sci. Eng., C*, 2018, **93**, 226–241, DOI: 10.1016/j.msec.2018.07.077.
- 155 M. A. Vandiver, B. R. Caire, J. R. Carver, K. Waldrop, M. R. Hibbs, J. R. Varcoe, A. M. Herring and M. W. Liberatore, Mechanical Characterization of Anion Exchange Membranes by Extensional Rheology under Controlled Hydration, *J. Electrochem. Soc.*, 2014, **161**, 10, DOI: 10.1149/2.0971410jes.
- 156 T. S. Zhao, K.-D. Kreuer and T. V. Nguyen, *Advances in Fuel Cells*, Elsevier, 1st edn, 2007, vol. 1.
- 157 R. C. T. Slade, J. P. Kizewski, S. D. Poynton, R. Zeng and J. R. Varcoe, Alkaline Membrane Fuel Cells, in *Fuel Cells: Selected Entries from the Encyclopedia of Sustainability Science and Technology*, ed. K.-D. Kreuer, Springer-Verlag, New York, 2013, vol. 1.
- 158 X. Wu, W. Chen, X. Yan, G. He, J. Wang, Y. Zhang and X. Zhu, Enhancement of hydroxide conductivity by the di-quaternization strategy for poly(ether ether ketone) based anion exchange membranes, *J. Mater. Chem. A*, 2014, **2**, 12222–12231, DOI: 10.1039/c4ta01397b.
- 159 M. A. Hickner, A. M. Herring and E. B. Coughlin, Anion exchange membranes: Current status and moving forward, *J. Polym. Sci., Part B: Polym. Phys.*, 2013, **52**(4), DOI: 10.1002/polb.23431.
- 160 K. Yoshimura, S. Yamaguchi, H. Tanaka, S. Warapon, H. Shishitani, B.-S. Ko and Y. Maekawa, Basicity-dependent properties of anion conducting membranes consisting of iminium cations for alkaline fuel cells, *J. Polym. Sci., Part A: Polym. Chem.*, 2018, **57**, 503–510, DOI: 10.1002/pola.29288.
- 161 N. Ziv and D. R. Dekel, A practical method for measuring the true hydroxide conductivity of anion exchange membranes, *Electrochem. Commun.*, 2018, **88**, 109–113, DOI: 10.1016/j.elecom.2018.01.021.
- 162 T. M. Lim, M. Ulaganathan and Q. Yan, *Advances in membrane and stack design of redox flow batteries (RFBs) for medium- and large-scale energy storage*, Elsevier Ltd., 2014, DOI: 10.1016/B978-1-78242-013-2.00014-5.
- 163 F. Karas, J. Hnát, M. Paidar, J. Schauer and K. Bouzek, Determination of the ion-exchange capacity of anion-selective membranes, *Int. J. Hydrogen Energy*, 2014, **39**, 5054–5062, DOI: 10.1016/j.ijhydene.2014.01.074.
- 164 B. C. Ong, S. K. Kamarudin and S. Basri, Direct liquid fuel cells: A review, *Int. J. Hydrogen Energy*, 2017, **42**, 10142–10157, DOI: 10.1016/j.ijhydene.2017.01.117.
- 165 J. R. Varcoe and R. C. T. Slade, Prospects for alkaline anion-exchange membranes in low temperature fuel cells, *Fuel Cells*, 2005, **5**, 187–200, DOI: 10.1002/face.200400045.
- 166 Y. Lu, A. A. Armentrout, J. Li, H. L. Tekinalp, J. Nanda and S. Ozcan, A cellulose nanocrystal-based composite electrolyte with superior dimensional stability for alkaline fuel cell membranes, *J. Mater. Chem. A*, 2015, **3**, 13350–13356, DOI: 10.1039/C5TA02304A.
- 167 Z. Sun, B. Lin and F. Yan, Anion-Exchange Membranes for Alkaline Fuel-Cell Applications: The Effects of Cations, *ChemSusChem*, 2018, **11**, 58–70, DOI: 10.1002/cssc.201701600.
- 168 W. C. Ryan O’Hayre, S.-W. Cha and F. B. Prinz, *Fuel cell fundamentals*, John Wiley & Sons, 2016, DOI: 10.1017/CBO9781107415324.004.
- 169 J. Larminie and A. Dicks, *Fuel Cell systems Explained*, John Wiley & Sons, 2003, DOI: 10.1002/9781118878330.
- 170 S. Heysiattalab, M. Shakeri, M. Safari and M. M. Keikha, Investigation of key parameters influence on performance of direct ethanol fuel cell (DEFC), *J. Ind. Eng. Chem.*, 2011, **17**, 727–729, DOI: 10.1016/j.jiec.2011.05.037.
- 171 D. C. Spiegel, *Polarization curves*, 2017.
- 172 Y.-J. Wang, J. Qiao, R. Baker and J. Zhang, Alkaline polymer electrolyte membranes for fuel cell applications, *Chem. Soc. Rev.*, 2013, **42**(13), 5768–5787, DOI: 10.1039/c3cs60053j.
- 173 Hydrogen and fuel cell technologies office, Office of energy efficiency & renewable energy, U.S. Department of Energy, *DOE Technical Targets for Polymer Electrolyte Membrane Fuel Cell Components*, accessed August 21, 2020, <https://www.energy.gov/eere/fuelcells/doe-technical-targets-polymer-electrolyte-membrane-fuel-cell-components#mea>.
- 174 Hydrogen and fuel cell technologies office, Office of energy efficiency & renewable energy, U.S. Department of Energy, *Fuel Cells*, accessed August 21, 2020, <https://www.energy.gov/eere/fuelcells/fuel-cells>.
- 175 D. R. Dekel, I. G. Rasin and S. Brandon, Predicting performance stability of anion exchange membrane fuel cells, *J. Power Sources*, 2019, **420**, 118–123, DOI: 10.1016/j.jpowsour.2019.02.069.
- 176 J. Maya-Cornejo, R. Carrera-Cerritos, D. Sebastián, J. Ledesma-García, L. G. Arriaga, A. S. Aricò and V. Baglio, PtCu catalyst for the electro-oxidation of ethanol in an alkaline direct alcohol fuel cell, *Int. J. Hydrogen Energy*, 2017, **42**, 27919–27928, DOI: 10.1016/j.ijhydene.2017.07.226.
- 177 L. An, T. S. Zhao, S. Y. Shen, Q. X. Wu and R. Chen, Performance of a direct ethylene glycol fuel cell with an anion-exchange membrane, *Int. J. Hydrogen Energy*, 2010, **35**, 4329–4335, DOI: 10.1016/j.ijhydene.2010.02.009.
- 178 K. T. Møller, T. R. Jensen, E. Akiba and H. wen Li, Hydrogen - A sustainable energy carrier, *Prog. Nat. Sci.: Mater. Int.*, 2017, **27**, 34–40, DOI: 10.1016/j.pnsc.2016.12.014.
- 179 M. Dresselhaus and I. Thomas, Alternative energy technologies, *Nature*, 2001, **414**, 332–337, DOI: 10.1038/35104599.





- 180 C. E. Commission, *California Air Resources Board, Assessment of Time and Cost Needed to Attain 100 Hydrogen Refueling Stations in California*, 2015, p. 7.
- 181 S. P. S. Badwal, S. Giddey, A. Kulkarni, J. Goel and S. Basu, Direct ethanol fuel cells for transport and stationary applications - A comprehensive review, *Appl. Energy*, 2015, **145**, 80–103, DOI: 10.1016/j.apenergy.2015.02.002.
- 182 E. H. Yu, X. Wang, U. Krewer, L. Li and K. Scott, Direct oxidation alkaline fuel cells: From materials to systems, *Energy Environ. Sci.*, 2012, **5**, 5668–5680, DOI: 10.1039/c2ee02552c.
- 183 Z. Zakaria and S. K. Kamarudin, Performance of quaternized poly(vinyl alcohol)-based electrolyte membrane in passive alkaline DEFCs application: RSM optimization approach, *J. Appl. Polym. Sci.*, 2019, **47526**, 1–18, DOI: 10.1002/app.47526.
- 184 S. N. T. Z. Zakaria and S. K. Kamarudin, Influence of Graphene Oxide on the Ethanol Permeability and Ionic Conductivity of QPVA-Based Membrane in Passive Alkaline Direct Ethanol Fuel Cells, *Nanoscale Res. Lett.*, 2019, **14**, 28, DOI: 10.1186/s11671-018-2836-3.
- 185 X. Fuku, M. Modibedi, N. Matinise, P. Mokoena, N. Xaba and M. Mathe, Single step synthesis of bio-inspired NiO/C as Pd support catalyst for dual application: Alkaline direct ethanol fuel cell and CO<sub>2</sub> electro-reduction, *J. Colloid Interface Sci.*, 2019, **545**, 138–152, DOI: 10.1016/j.jcis.2019.03.030.
- 186 D. Herranz, C. Palacio, R. Escudero-Cid, E. Fatás, P. Ocón and M. Montiel, Poly (vinyl alcohol) and poly(benzimidazole) blend membranes for high performance alkaline direct ethanol fuel cells, *Renewable Energy*, 2018, **127**, 883–895, DOI: 10.1016/j.renene.2018.05.020.
- 187 L. Ma, H. He, A. Hsu and R. Chen, PdRu/C catalysts for ethanol oxidation in anion-exchange membrane direct ethanol fuel cells, *J. Power Sources*, 2013, **241**, 696–702, DOI: 10.1016/j.jpowsour.2013.04.051.
- 188 A. Dutta and J. Datta, Outstanding catalyst performance of PdAuNi nanoparticles for the anodic reaction in an alkaline direct ethanol (with anion-exchange membrane) fuel cell, *J. Phys. Chem. C*, 2012, **116**, 25677–25688, DOI: 10.1021/jp305323s.
- 189 Y. S. Li, Y. L. He and W. W. Yang, Performance characteristics of air-breathing anion-exchange membrane direct ethanol fuel cells, *Int. J. Hydrogen Energy*, 2013, **38**, 13427–13433, DOI: 10.1016/j.ijhydene.2013.07.042.
- 190 N. Fujiwara, Z. Siroma, S.-i. Yamazaki, T. Ioroi, H. Senoh and K. Yasuda, Direct ethanol fuel cells using an anion exchange membrane, *J. Power Sources*, 2008, **185**, 621–626, DOI: 10.1016/j.jpowsour.2008.09.024.
- 191 J. M. Ogden, M. M. Steinbugler and T. G. Kreutz, A comparison of hydrogen, methanol and gasoline as fuels for fuel cell vehicles: implications for vehicle design and infrastructure development, *J. Power Sources*, 1999, **79**, 143–168.
- 192 T. S. Zhao, Y. S. Li and S. Y. Shen, Anion-exchange membrane direct ethanol fuel cells: Status and perspective, *Front. Energy Power Eng. China.*, 2010, **4**, 443–458, DOI: 10.1007/s11708-010-0127-5.
- 193 C.-A. Racovitză, Bio-Ethanol Used in Engines and in the Fuel Cells, *Bul. Inst. Politeh. Iasi*, 2010, **56**, 345–351.
- 194 J. T. C. Cremers, D. Bayer, B. Kintzel, M. Joos, F. Jung and M. Krausa, Oxidation of Alcohols in Acidic and Alkaline Environments, *ECS Trans.*, 2008, **16**, 1263–1273, DOI: 10.1149/1.2981967.
- 195 C. A. Cardona and Ó. J. Sánchez, Fuel ethanol production: Process design trends and integration opportunities, *Bioresour. Technol.*, 2007, **98**, 2415–2457, DOI: 10.1016/j.biortech.2007.01.002.
- 196 R. Harun, J. W. S. Yip, S. Thiruvankadam, W. A. W. A. K. Ghani, T. Cherrington and M. K. Danquah, Algal biomass conversion to bioethanol—a step-by-step assessment, *Biotechnol. J.*, 2014, **9**, 73–86, DOI: 10.1002/biot.201200353.
- 197 T. Jurzinsky, R. Bär, C. Cremers, J. Tübke and P. Elsner, Highly active carbon supported palladium-rhodium Pd<sub>x</sub>Rh/C catalysts for methanol electrooxidation in alkaline media and their performance in anion exchange direct methanol fuel cells (AEM-DMFCs), *Electrochim. Acta*, 2015, **176**, 1191–1201, DOI: 10.1016/j.electacta.2015.07.176.
- 198 T. Jurzinsky, C. Cremers, F. Jung, K. Pinkwart and J. Tübke, Development of materials for anion-exchange membrane direct alcohol fuel cells, *Int. J. Hydrogen Energy*, 2015, **40**, 11569–11576, DOI: 10.1016/j.ijhydene.2015.02.056.
- 199 T. Jurzinsky, R. Bär, N. Heppel, C. Cremers and J. Tübke, A comb-like ionomer based on poly(2,6-dimethyl-1,4-phenylene oxide) for the use as anodic binder in anion-exchange membrane direct methanol fuel cells, *Solid State Ionics*, 2017, **303**, 1–11, DOI: 10.1016/j.ssi.2016.12.036.
- 200 Y. S. Ye, M. Y. Cheng, X. L. Xie, J. Rick, Y. J. Huang, F. C. Chang and B. J. Hwang, Alkali doped polyvinyl alcohol/graphene electrolyte for direct methanol alkaline fuel cells, *J. Power Sources*, 2013, **239**, 424–432, DOI: 10.1016/j.jpowsour.2013.03.021.
- 201 X. He, J. Liu, H. Zhu, Y. Zheng and D. Chen, Novel quaternary ammonium functional addition-type norbornene copolymer as hydroxide-conductive and durable anion exchange membrane for direct methanol fuel cells, *RSC Adv.*, 2015, **5**, 63215–63225, DOI: 10.1039/c5ra09393g.
- 202 A. Serov and C. Kwak, Direct hydrazine fuel cells: A review, *Appl. Catal., B*, 2010, **98**, 1–9, DOI: 10.1016/j.apcatb.2010.05.005.
- 203 J. A. Harrison and Z. A. Khan, The oxidation of hydrazine in alkaline solution at platinum and mercury, *J. Electroanal. Chem.*, 1970, **26**, 1–11, DOI: 10.1016/S0022-0728(70)80060-2.
- 204 K. Yoshimura, H. Koshikawa, T. Yamaki, H. Shishitani, K. Yamamoto, S. Yamaguchi, H. Tanaka and Y. Maekawa, Imidazolium Cation Based Anion-Conducting Electrolyte Membranes Prepared by Radiation Induced Grafting for



- Direct Hydrazine Hydrate Fuel Cells, *J. Electrochem. Soc.*, 2014, **161**, F889–F893, DOI: 10.1149/2.0511409jes.
- 205 H. Qin, Z. Liu, Y. Guo and Z. Li, The affects of membrane on the cell performance when using alkaline borohydride-hydrazine solutions as the fuel, *Int. J. Hydrogen Energy*, 2010, **35**, 2868–2871, DOI: 10.1016/j.ijhydene.2009.05.004.
- 206 A. López-Coronel, E. Ortiz-Ortega, L. J. Torres-Pacheco, M. Guerra-Balcázar, L. G. Arriaga, L. Álvarez-Contreras and N. Arjona, High performance of Pd and PdAg with well-defined facets in direct ethylene glycol microfluidic fuel cells, *Electrochim. Acta*, 2019, **320**(10), 134622, DOI: 10.1016/j.electacta.2019.134622.
- 207 L. An and R. Chen, Recent progress in alkaline direct ethylene glycol fuel cells for sustainable energy production, *J. Power Sources*, 2016, **329**, 484–501, DOI: 10.1016/j.jpowsour.2016.08.105.
- 208 L. Xin, Z. Zhang, J. Qi, D. Chadderdon and W. Li, Electrocatalytic oxidation of ethylene glycol (EG) on supported Pt and Au catalysts in alkaline media: Reaction pathway investigation in three-electrode cell and fuel cell reactors, *Appl. Catal., B*, 2012, **125**, 85–94, DOI: 10.1016/j.apcatb.2012.05.024.
- 209 L. An, L. Zeng and T. S. Zhao, An alkaline direct ethylene glycol fuel cell with an alkali-doped polybenzimidazole membrane, *Int. J. Hydrogen Energy*, 2013, **38**, 10602–10606, DOI: 10.1016/j.ijhydene.2013.06.042.
- 210 Z. Zhang, L. Xin and W. Li, Supported gold nanoparticles as anode catalyst for anion-exchange membrane-direct glycerol fuel cell (AEM-DGFC), *Int. J. Hydrogen Energy*, 2012, **37**, 9393–9401, DOI: 10.1016/j.ijhydene.2012.03.019.
- 211 N. Benipal, J. Qi, J. C. Gentile and W. Li, Direct glycerol fuel cell with polytetrafluoroethylene (PTFE) thin film separator, *Renewable Energy*, 2017, **105**, 647–655, DOI: 10.1016/j.renene.2016.12.028.
- 212 Z. Wang, L. Xin, X. Zhao, Y. Qiu, Z. Zhang, O. A. Baturina and W. Li, Carbon supported Ag nanoparticles with different particle size as cathode catalysts for anion exchange membrane direct glycerol fuel cells, *Renewable Energy*, 2014, **62**, 556–562, DOI: 10.1016/j.renene.2013.08.005.
- 213 J. Ma, N. A. Choudhury and Y. Sahai, A comprehensive review of direct borohydride fuel cells, *Renewable Sustainable Energy Rev.*, 2010, **14**, 183–199, DOI: 10.1016/j.rser.2009.08.002.
- 214 H. Qin, L. Lin, W. Chu, W. Jiang, Y. He, Q. Shi, Y. Deng, Z. Ji, J. Liu and S. Tao, Introducing catalyst in alkaline membrane for improved performance direct borohydride fuel cells, *J. Power Sources*, 2018, **374**, 113–120, DOI: 10.1016/j.jpowsour.2017.11.008.
- 215 O. Siddiqui, H. Ishaq and I. Dincer, Experimental investigation of improvement capability of ammonia fuel cell performance with addition of hydrogen, *Energy Convers. Manage.*, 2020, **205**, 112372, DOI: 10.1016/j.enconman.2019.112372.
- 216 J. C. M. Silva, S. G. Silva, R. F. B. De Souza, G. S. Buzzo, E. V. Spinacé, A. O. Neto and M. H. M. T. Assumpc, PtAu/C electrocatalysts as anodes for direct ammonia fuel cell, *Appl. Catal., A*, 2015, **490**, 133–138, DOI: 10.1016/j.apcata.2014.11.015.
- 217 R. Lan and S. Tao, Ammonia as a Suitable Fuel for Fuel Cells, *Front. Energy Res.*, 2014, **2**, 3–6, DOI: 10.3389/fenrg.2014.00035.
- 218 S. Suzuki, H. Muroyama, T. Matsui and K. Eguchi, Fundamental studies on direct ammonia fuel cell employing anion exchange membrane, *J. Power Sources*, 2012, **208**, 257–262, DOI: 10.1016/j.jpowsour.2012.02.043.
- 219 O. Siddiqui and I. Dincer, Experimental investigation and assessment of direct ammonia fuel cells utilizing alkaline molten and solid electrolytes, *Energy*, 2019, **169**, 914–923, DOI: 10.1016/j.energy.2018.12.096.
- 220 M. H. M. T. Assumpção, S. G. R. F. B. da Silvade Souza, G. S. Buzzo, E. V. Spinacé, A. O. Neto and J. C. M. Silva, Direct ammonia fuel cell performance using PtIr/C as anode electrocatalysts, *Int. J. Hydrogen Energy*, 2014, **39**(10), 5148–5152, DOI: 10.1016/j.ijhydene.2014.01.053.
- 221 L. Du, S. Lou, G. Chen, G. Zhang, F. Kong, Z. Qian, C. Du, Y. Gao, S. Sun and G. Yin, Direct dimethyl ether fuel cells with low platinum-group-metal loading at anode: Investigations of operating temperatures and anode Pt/Ru ratios, *J. Power Sources*, 2019, **433**, 126690, DOI: 10.1016/j.jpowsour.2019.05.096.
- 222 K. Xu, S. J. Lao, H. Y. Qin, B. H. Liu and Z. P. Li, A study of the direct dimethyl ether fuel cell using alkaline anolyte, *J. Power Sources*, 2010, **195**, 5606–5609, DOI: 10.1016/j.jpowsour.2010.03.073.
- 223 H. A. Miller, J. Ruggeri, A. Marchionni, M. Bellini, M. V. Pagliaro, C. Bartoli, A. Pucci, E. Passaglia and F. Vizza, Improving the energy efficiency of direct formate fuel cells with a Pd/C-CeO<sub>2</sub> anode catalyst and anion exchange ionomer in the catalyst layer, *Energies*, 2018, **11**, 1–12, DOI: 10.3390/en11020369.
- 224 T. Q. Nguyen, D. Minami, C. Hua, A. Miller, K. Tran and J. L. Haan, Ambient Temperature Operation of a Platinum-Free Direct Formate Fuel Cell, *J. Fuel Cell Sci. Technol.*, 2015, **12**(1), 014501, DOI: 10.1115/1.4029072.
- 225 J. Jiang and A. Wieckowski, Prospective direct formate fuel cell, *Electrochem. Commun.*, 2012, **18**, 41–43, DOI: 10.1016/j.elecom.2012.02.017.
- 226 L. Zeng, Z. K. Tang and T. S. Zhao, A high-performance alkaline exchange membrane direct formate fuel cell, *Appl. Energy*, 2014, **115**, 405–410, DOI: 10.1016/j.apenergy.2013.11.039.
- 227 K. Tran, T. Q. Nguyen, A. M. Bartrom, A. Sadiki and J. L. Haan, A Fuel-Flexible Alkaline Direct Liquid Fuel Cell, *Fuel Cells*, 2014, **14**(6), DOI: 10.1002/face.201300291.
- 228 A. M. Bartrom, J. Ta, T. Q. Nguyen, J. Her, A. Donovan and J. L. Haan, Optimization of an anode fabrication method for the alkaline Direct Formate Fuel Cell, *J. Power Sources*, 2013, **229**, 234–238, DOI: 10.1016/j.jpowsour.2012.12.007.
- 229 M. E. P. Markiewicz and S. H. Bergens, Electro-oxidation of 2-propanol and acetone over platinum, platinum – ruthenium, and ruthenium nanoparticles in alkaline electrolytes, *J. Power Sources*, 2008, **185**(1), 222–225, DOI: 10.1016/j.jpowsour.2008.06.023.



- 230 M. E. P. Markiewicz and S. H. Bergens, A liquid electrolyte alkaline direct 2-propanol fuel cell, *J. Power Sources*, 2010, **195**, 7196–7201, DOI: 10.1016/j.jpowsour.2010.05.017.
- 231 H. Y. Wolf Vielstich and H. A. Gasteiger, *Handbook of Fuel Cells: Advances in Electrocatalysis, Materials, Diagnostics and Durability*, John Wiley & Sons, 2009.
- 232 E. Drioli, L. Giorno, E. Fontananova, *Comprehensive Membrane Science and Engineering*, Elsevier, 2nd edn, 2017.
- 233 T. S. Z. Liang, *An, Anion Exchange Membrane Fuel Cells: Principles, Materials and Systems*, 2018.
- 234 Z. F. Pan, L. An, T. S. Zhao and Z. K. Tang, Advances and challenges in alkaline anion exchange membrane fuel cells, *Prog. Energy Combust. Sci.*, 2018, **66**, 141–175, DOI: 10.1016/j.pecs.2018.01.001.
- 235 W. You, K. J. T. Noonan and G. W. Coates, Alkaline-stable anion exchange membranes: A review of synthetic approaches, *Prog. Polym. Sci.*, 2020, **100**, 101177, DOI: 10.1016/j.procpolymsci.2019.101177.

